The Swinging Spring: A Simple Model of Atmospheric Balance

Peter Lynch, Met Éireann, Dublin, Ireland

This simple system looks like a toy at best, but its behaviour is astonishingly complex, with many facets of more than academic lustre (*Breitenberger and Mueller, 1981*).

1 Introduction

1.1 Résumé

The linear normal modes of the atmosphere fall into two categories, the low frequency Rossby waves and the high frequency gravity waves. The elastic pendulum is a simple mechanical system having low frequency and high frequency oscillations. Its motion is governed by four coupled nonlinear ordinary differential equations. We study the dynamics of this system, drawing analogies between its behaviour and that of the atmosphere. The linear normal mode structure of the system is analysed, the procedure of initialization is described and the existence and character of the slow manifold is discussed.

1.2 Prologue

The concepts of initialization, filtering and the slow manifold can be clearly illustrated by considering the dynamics of a simple mechanical system governed by a set of ordinary differential equations. The elastic pendulum or swinging spring depicted in Fig. 1 comprises a heavy bob suspended by a light elastic spring which may stretch but not bend. The bob is free to move in a vertical plane. The oscillations of this system are of two types, distinguished by their physical restoring mechanisms. For an appropriate choice of parameters, the elastic oscillations have much higher frequency than the rotation or libration of the bob. We consider the elastic oscillations to be analogues of the high frequency gravity waves in the atmosphere. Similarly, the low frequency rotational motions are considered to correspond to the rotational or Rossby-Haurwitz waves. We will refer to the elastic and rotational motions as "fast" and "slow" respectively.

The linear analysis of this mechanical system is straightforward. When nonlinear effects are included there is coupling between the two types of motion,

and analytical methods are incapable of providing the solution. To obtain insight into the characteristics of the motion in this case we must turn to some powerful and general results from dynamical systems theory. The pendulum equations contain a small parameter, ϵ, the ratio of the frequencies of the slow and fast oscillations. The problem may be formulated in terms of a perturbed Hamiltonian, the size of the perturbation depending on ϵ. Then the Kolmogorov-Arnold-Moser or KAM theorem implies certain restraints on the nature of the solution. The validity of the conclusions drawn will be supported by numerical simulations.

Lorenz (1986) constructed a highly simplified model, comprising five ordinary differential equations, based on a truncated spectral expansion of the shallow water equations. He identified the variables corresponding to the high frequency oscillations as representing the gravity wave activity and defined the slow manifold to be an invariant sub-manifold of the five-dimensional phase space in which high frequency oscillations are permanently absent. In Bokhove and Shepherd (1996: BS96) Lorenz's model is further reduced, to a system of four ordinary differential equations. A similar reduction is made by Camassa (1995). These equations are structurally similar to the equations for a nonlinear pendulum coupled to a linear harmonic oscillator. The system is amenable to the application of Hamiltonian perturbation theory. For small values of the perturbation or coupling parameter, one may identify an invariant manifold on which the high frequency activity is unequivocally zero. This manifold is nonlinearly stable: a small gravity wave disturbance about it will remain permanently bounded. However, the manifold is not defined continuously throughout phase space, but is fractal (actually, Cantor-like) in structure. Numerical experiments in BS96 showed that, as the perturbation parameter increases, the extent of the manifold decreases until, ultimately, it disappears entirely.

It turns out that the simple mechanical system considered in this report is governed by mathematical equations having a structure very similar to Lorenz's model. Both can be described in terms of a system with two modes of behaviour, a linear harmonic oscillator and a nonlinear pendulum. The precise details of the coupling between the oscillator and pendulum differ in the two cases; but the conclusions of the KAM theorem do not depend upon these details. Therefore, much of the discussion in BS96—in particular, their conclusions about the existence of a slowest invariant manifold—can be applied directly to the elastic pendulum considered herein.

1.3 Outline of Contents

In Section 2 the Hamiltonian equations for the elastic pendulum are set down. The linear solutions are examined and the procedures for linear and nonlinear initialization are discussed. The concept of the slow manifold is introduced and illustrated by some numerical integrations. In Section 3 the ideas underly-

ing the KAM theorem are presented and its main conclusions are summarised. Some general consequences of the theorem—in celestial mechanics, particle physics and statistical mechanics—are briefly described. The application of KAM to the elastic pendulum occupies Section 4. The implications for the existence of a slow manifold for this system are discussed. We conclude that, for small values of the frequency ratio ϵ, it is possible, for almost all values of the slow variables, to define appropriate values of the fast variables in such a way that the solution has no high frequency oscillations. The exceptional cases give the slow manifold a fractal structure; but, for small ϵ, they form a set of negligible measure. These conclusions are supported by numerical experiments which are described in Section 5. Poincaré sections showing regions of regular motion and regions of chaos are plotted. For small ϵ the solutions are predominantly regular and the core solution representing purely slow motion can be clearly seen. As ϵ grows the solutions become more complex, until a stage is reached where the distinction between fast and slow time scales no longer makes sense. In Section 6 we digress to consider the case of resonance when the fast and slow time scales are in the ratio two-to-one, and show how energy is transformed back and forth periodically between the swinging and springing modes. In the final part of the paper, Section 7, we discuss miscellaneous aspects of the problem and touch upon some unresolved issues.

1.4 Previous Studies

The earliest substantial paper on the elastic pendulum seems to have been that of Vitt and Gorelik (1933). This study was motivated by the value of the system as a simple classical analogue for the quantum phenomenon of Fermi resonance in the infra-red spectrum of carbon dioxide. The paper discusses the recurrence phenomenon in which energy is converted back and forth between the elastic and pendular modes. A perturbation analysis led the authors to the discovery of two special "purely periodic" solutions with parabolic trajectories, for which the energy transfer vanishes, and to a formula for the period of recurrence in terms of an elliptic integral.

Heinbockel and Struble (1963) derived asymptotic solutions for small amplitude in both the resonant and non-resonant cases. They showed that for resonance the amplitude envelope is expressible in terms of Jacobian elliptic functions. They derived an expression for the range for which resonance occurs, showing how it increases with increasing energy. They also identified, but did not discuss, special solutions for which energy transfer vanishes (these particular solutions are the parabolic orbits of Vitt and Gorelik). Van der Burgh (1968) employed the asymptotic method of Krylov, Bogoliubov and Mitropolsky to analyse the small amplitude motions. He derived a single equation for the amplitude of the spring motion and deduced explicit expressions for the trajectories of the slow amplitudes. He showed that when the initial energy is predominantly elastic the period of vacillation is inversely proportional to the

amplitude. His analytical results were compared with analog computations. Kane and Kahn (1968) used Floquet theory to derive a criterion for resonance for a general class of systems which includes the elastic pendulum. They carried out a perturbation analysis based on the Hamilton-Jacobi equation to study the character of the resonant solutions. They confirmed their results by means of numerical integration of the full nonlinear equations.

Nayfeh (1973) re-examined the resonance phenomenon for the elastic pendulum — which he called the swinging spring — from several points of view. He considered the canonical variable approach of Kane and Kahn, 1968 (p 185), applied the method of Lie transforms (p 214) and performed a perturbation analysis using the method of multiple time-scales (p 262). However, his interest was primarily in illustrating the different perturbation methods and he did not go beyond the point of deriving equations for the slowly varying amplitudes. Breitenberger and Mueller (1981), in a comprehensive study, applied the 'slow fluctuation' technique: they introduced a canonical transformation to action-angle variables, developed the interaction term as a trigonometric series and kept only the slowly-varying part. This is equivalent to the averaged Hamiltonian technique (Nayfeh, 1973, p185). They showed that there are two constants of the motion and derived explicit solutions in terms on elliptic integrals. Their perturbation solutions were shown to have high accuracy compared to numerical solutions of the unapproximated system.

Núñez-Yépez *et al.* (1990) examine by numerical means the onset of chaos in an extensible pendulum at resonance. They find that for very small or very large total energy the motion is regular, but for a broad intermediate range of energies it is chaotic. They present their results in terms of Poincaré sections and maximum Lyapunov exponents. Cuerno *et al.* (1992) provide a good introduction to the study of regular and chaotic motions of the elastic pendulum. They discuss the applicability of the KAM theorem to this system, and confirm their speculations with numerical results. They show how the motion can be characterised by studying several indicators in combination. These are the Poincaré section, the maximum Lyapunov exponent, the autocorrelation function and the power spectrum. Simultaneous use of these four indicators is useful, as they serve to complement each other. Aničin *et al.* (1993) outline the phenomenon of parametric resonance and present arguments that this occurs only in one case, $\omega_{\mathrm{E}} = 2\omega_{\mathrm{R}}$. They use the Ince-Strutt diagram of instabilities of the Mathieu equation to show how the parameter range for instability and the growth-rate depend on the amplitude. Carretero-González *et al.* (1994) present a good general discussion on chaos in Hamiltonian systems. They discuss the resonance of the elastic pendulum as an analogue for the quantum phenomenon of Fermi resonance of triatomic molecules. They illustrate the regular and chaotic behaviour of the system by numerical integrations, discussing the results in terms of Poincaré sections, Liapunov exponents and autocorrelation functions.

In Banerjee and Bajaj (1996), a general set of four first-order amplitude equations, valid for any forced, damped system with two degrees of freedom, is derived by the method of averaging. The parameter range for which chaotic dynamics exists, is calculated using Melnikov's method, a global perturbation technique. The results are discussed in the context of a damped, forced system equivalent ot that of Georgiou and Schwartz (1996). Davidović *et al.* (1996) briefly review a large number of earlier papers on the elastic pendulum. They investigate the libration limits of the pendulum in exact resonance by using parabolic coordinates. They show that the representative point in coordinate space is confined within a lemon-shaped or crescent-shaped region (depending on the initial conditions) whose boundary is defined by three parabolae.

Several books which provided valuable background information for this study should be mentioned. *Newton's Clock: Chaos in the Solar System*, by Ivars Peterson (1993), is a general history of the study of planetary stability since ancient times, with emphasis on recent developments. *Celestial Encounters: the Origins of Chaos and Stability*, by Florin Diacu and Philip Holmes (1996), tells the fascinating story of how chaos theory emerged, starting with Poincaré's dramatic discoveries in celestial mechanics, and including an excellent chapter on KAM theory. *The Genesis of Simulation in Dynamics: Pursuing the Fermi-Pasta-Ulam Problem*, by Thomas P. Weissert (1997), reviews the influence of the FPU problem on the development of dynamical systems theory and discusses how the KAM theorem bears on the surprising results of Fermi, *et al.* Michael Berry's review paper, *Regular and irregular motion*, provides an accessible, comprehensive introduction to KAM. Of numerous textbooks on modern dynamics, the following were found to be especially useful: Jackson's (1991) *Perspectives of Nonlinear Dynamics*, Lichtenberg and Lieberman's (1992) *Regular and Chaotic Dynamics*, Ott's (1993) *Chaos in Dynamical Systems* and Tabor's (1989) *Chaos and Integrability in Nonlinear Dynamics.*

2 The Dynamic Equations for the Elastic Pendulum

2.1 The Hamiltonian Equations

Let ℓ_0 be the unstretched length of the spring, k its elasticity or stiffness and m the mass of the bob. At equilibrium (Fig. 1(a)) the elastic restoring force is balanced by the weight

$$k(\ell - \ell_0) = mg \qquad \text{or} \qquad \ell = \ell_0 \left(1 + \frac{mg}{k\ell_0}\right) . \tag{1}$$

It is convenient to write the dynamic equations in Hamilton's canonical form. If the total energy H is expressed in terms of the coordinates q_n and momenta

p_n, these equations are

$$\frac{dq_n}{dt} = \frac{\partial H}{\partial p_n}, \qquad \frac{dp_n}{dt} = -\frac{\partial H}{\partial q_n}. \tag{2}$$

In the present case polar coordinates $q_r = r$ and $q_\theta = \theta$ are used, and the radial and angular momenta are $p_r = m\dot{r}$ and $p_\theta = mr^2\dot{\theta}$. The total energy is a sum of kinetic, elastic potential and gravitational potential energy:

$$H = \frac{1}{2m}\left(p_r^2 + \frac{p_\theta^2}{r^2}\right) + \tfrac{1}{2}k(r-\ell_0)^2 - mgr\cos\theta\,. \tag{3}$$

The dynamical equations (2) may now be written explicitly

$$\begin{aligned}
\dot{\theta} &= p_\theta/mr^2 && \text{(4a)}\\
\dot{p}_\theta &= -mgr\sin\theta && \text{(4b)}\\
\dot{r} &= p_r/m && \text{(4c)}\\
\dot{p}_r &= p_\theta^2/mr^3 - k(r-\ell_0) + mg\cos\theta && \text{(4d)}
\end{aligned}$$

These equations may also be written symbolically in vector form

$$\dot{\mathbf{X}} + \mathbf{L}\mathbf{X} + \mathbf{N}(\mathbf{X}) = 0 \tag{5}$$

where $\mathbf{X} = (\theta, p_\theta, r, p_r)^{\mathrm{T}}$, $\mathbf{L}$ is the matrix of coefficients of the linear terms and $\mathbf{N}$ is a nonlinear vector function. The state vector $\mathbf{X}$ specifies a point in phase space (here, 4-dimensional) which defines the state of the system at any time; the motion is represented by the trajectory traced out by $\mathbf{X}$ as it moves through phase space.

2.2 Linear Normal Modes

Let us now suppose that the amplitude of the motion is small, so that $|r'| = |r-\ell| \ll \ell$ and $|\theta| \ll 1$. The equations may be linearized and written in matrix form

$$\frac{d}{dt}\begin{pmatrix}\theta\\ p_\theta\\ r'\\ p_r\end{pmatrix} = \begin{pmatrix}0 & 1/m\ell^2 & 0 & 0\\ -mg\ell & 0 & 0 & 0\\ 0 & 0 & 0 & 1/m\\ 0 & 0 & -k & 0\end{pmatrix}\begin{pmatrix}\theta\\ p_\theta\\ r'\\ p_r\end{pmatrix} \tag{6}$$

We see clearly how the matrix is block-diagonal so that the equations split into two subsystems. The state vector $\mathbf{X}$ is comprised of two sub-vectors:

$$\mathbf{X} = \begin{pmatrix}\mathbf{Y}\\ \mathbf{Z}\end{pmatrix}, \qquad \text{where} \quad \mathbf{Y} = \begin{pmatrix}\theta\\ p_\theta\end{pmatrix} \quad \text{and} \quad \mathbf{Z} = \begin{pmatrix}r'\\ p_r\end{pmatrix},$$

and the linear dynamics of these components evolve independently:

$$\dot{\mathbf{Y}} = \begin{pmatrix} 0 & 1/m\ell^2 \\ -mg\ell & 0 \end{pmatrix} \mathbf{Y}\,, \qquad \dot{\mathbf{Z}} = \begin{pmatrix} 0 & 1/m \\ -k & 0 \end{pmatrix} \mathbf{Z}\,.$$

We call the motion described by $\mathbf{Y}$ the rotational component and that described by $\mathbf{Z}$ the elastic component. The rotational equations may be combined to yield

$$\ddot{\theta} + (g/\ell)\theta = 0 \tag{7a}$$

which is the equation for a simple (anelastic) pendulum having oscillatory solutions with frequency $\sqrt{g/\ell}$. The remaining two equations yield

$$\ddot{r}' + (k/m)r' = 0\,, \tag{7b}$$

the equations for elastic oscillations with frequency $\sqrt{k/m}$. The solutions of (7a) and (7b) are called the linear normal modes. We define the rotational and elastic frequencies and their ratio by

$$\omega_{\mathrm{R}} = \sqrt{\frac{g}{\ell}}\,, \qquad \omega_{\mathrm{E}} = \sqrt{\frac{k}{m}}\,, \qquad \epsilon \equiv \left(\frac{\omega_{\mathrm{R}}}{\omega_{\mathrm{E}}}\right)\,.$$

It follows from (1) that the rotational frequency is always less than the elastic:

$$\epsilon^2 = \frac{mg}{k\ell} = \left(1 - \frac{\ell_0}{\ell}\right) < 1\,, \qquad \text{so that} \qquad |\omega_{\mathrm{R}}| < |\omega_{\mathrm{E}}|\,. \tag{8}$$

Except in §6 below, we assume that the parameters are such that $\epsilon \ll 1$. Then $\ell \approx \ell_0$, and we define $\epsilon_0 \equiv \sqrt{mg/k\ell_0}$, noting that

$$\epsilon_0^2 = \frac{mg}{k\ell_0} = \left(\frac{\epsilon^2}{1-\epsilon^2}\right) \approx \epsilon^2\,.$$

In this case the linear normal modes are clearly distinct: the rotational mode has low frequency (LF) and the elastic mode has high frequency (HF).

2.3 Linear and Nonlinear Initialization

For small amplitude motions, for which the nonlinear terms are negligible, the LF and HF oscillations are completely independent of each other and evolve without interaction. We can suppress the HF component completely by setting its initial amplitude to zero:

$$\mathbf{Z} = \begin{pmatrix} r' \\ p_r \end{pmatrix} = \mathbf{0} \quad \text{at} \quad t = 0\,.$$

This procedure is called linear initialization. When the amplitude is large, nonlinear terms are no longer negligible and the LF and HF motions interact.

It is clear from the equations (4) that linear initialization will not ensure permanent absence of HF motions: the nonlinear LF terms generate radial momentum. Machenhauer (1977) proposed an effective means of minimizing HF oscillations in such systems: set the initial *tendency* of the HF components to zero:

$$\dot{\mathbf{Z}} = \begin{pmatrix} \dot{r} \\ \dot{p}_r \end{pmatrix} = \mathbf{0} \quad \text{at} \quad t = 0\,, \tag{9}$$

This procedure is called nonlinear initialization. For the pendulum, we can deduce explicit expressions for the initial conditions by using (9) in (4c) and (4d):

$$r(0) = r_{\mathrm{B}} \equiv \frac{\ell_0(1+\epsilon_0^2\cos\theta)}{1-(\dot{\theta}/\omega_{\mathrm{E}})^2}\,, \qquad p_r(0) = 0\,. \tag{10}$$

Thus, given arbitrary initial conditions $\mathbf{X} = (\theta, p_\theta, r, p_r)^{\mathrm{T}}$, we replace $\mathbf{Z} = (r, p_r)^{\mathrm{T}}$ by $\mathbf{Z}_{\mathrm{B}} = (r_{\mathrm{B}}, 0)^{\mathrm{T}}$. The rotational component $\mathbf{Y} = (\theta, p_\theta)^{\mathrm{T}}$ remains unchanged. If, for simplicity, we assume that the angular momentum p_θ vanishes at $t = 0$, the condition $r = r_{\mathrm{B}}$ defines a curve in the (r, θ)-plane:

$$r = \ell_0(1+\epsilon_0^2\cos\theta)\,. \tag{11}$$

This is one of the classical 'special curves', called the limaçon of Pascal, named after Étienne, father of Blaise Pascal (Wells, 1991). A set of such curves, for a selection of values of ϵ_0 is shown in Fig. 2.

2.4 The Slow Manifold and the Slow Equations

The linear initialization condition $\mathbf{Z} = \mathbf{0}$ defines a two-dimensional subspace of phase-space, the plane surface $\mathcal{Y}$ through the origin given by $r = p_r = 0$. The full space is a direct sum of linear slow and fast spaces, $\mathcal{Y} \oplus \mathcal{Z}$. For purely linear motion, points in the subspace $\mathcal{Y}$ will remain in it. However, for nonlinear motion a point initially in this plane will not remain therein. The nonlinear initialization condition $\dot{\mathbf{Z}} = \mathbf{0}$ defines a two-dimensional nonlinear subset, the surface $\mathcal{S}_1$ given by $r = r_{\mathrm{B}}$, $p_r = 0$. We say that the fast variables are slaved to the slow ones by $r = r_{\mathrm{B}}(\theta, p_\theta)$ and $p_r = 0$. The surface $\mathcal{S}_1$ may be considered as a first-order approximation to the *slow manifold* (Leith, 1980). The slow manifold, $\mathcal{S}$, is a putative invariant sub-manifold of total phase space, of lower dimension than the full space, upon which solutions are constrained to evolve free from high-frequency oscillations. The primary goal of initialization is to find a point which is close both to the manifold $\mathcal{S}$ and to the given initial data. While a point initially on $\mathcal{S}_1$ is not guaranteed to remain on it, we find that points initially close to $\mathcal{S}_1$ remain close to it for all time: $\mathcal{S}_1$ acts like a guiding centre for the motion. Nonlinear initialization ensures that the initial point is on $\mathcal{S}_1$. In the case of the elastic pendulum the manifold $\mathcal{S}_1$ can be represented as a surface in three-space, since $p_r = 0$ (see Fig. 3). The cross-section through the plane $p_\theta = 0$ is the limaçon $r =$

$\ell_0(1+\epsilon_0^2\cos\theta)$. Limaçon, meaning snail, is a happily apposite appellation for a curve circumscribing the slow manifold.

We can impose the condition that the motion evolves on the manifold $\mathcal{S}_1$ by modifying, or filtering, the dynamical equations. We replace the prognostic equations for the radial motion by the diagnostic equations $\dot{\mathbf{Z}} = \mathbf{0}$ or $\mathbf{Z} = \mathbf{Z}_\mathrm{B}$. This yields the slow equations (Daley, 1980; Lynch, 1989). The system becomes

$$\begin{aligned} \dot\theta &= p_\theta/mr^2 && \text{(12a)}\\ \dot p_\theta &= -mgr\sin\theta && \text{(12b)}\\ 0 &= p_r/m && \text{(12c)}\\ 0 &= p_\theta^2/mr^3 - k(r-\ell_0) + mg\cos\theta && \text{(12d)} \end{aligned}$$

The slow equations have linear normal mode solutions corresponding to the rotational motions, with frequency $\omega_\mathrm{R} = \sqrt{g/\ell_0}$. There are no HF normal modes; they have been filtered out by the condition $\dot{\mathbf{Z}} = \mathbf{0}$. The slow equations describe dynamics on the manifold $\mathcal{S}_1$. It must be stressed that the solutions of this system are not an exact representation of the dynamics of the elastic pendulum, but they are a close approximation to the full dynamics provided ϵ_0 is small (so that the omitted terms are negligible) and the amplitude of the HF component is small (so that the trajectory remains close to $\mathcal{S}_1$).

2.5 Numerical Solutions

We shall further elucidate the dynamics of the elastic pendulum by presenting results of numerical integrations of the governing equations (4) and of their 'slow' counterparts (12). The parameter values are $m = 1\,\mathrm{kg}$, $\ell_0 = 1\,\mathrm{m}$, $g = \pi^2\,\mathrm{m\,s^{-2}}$ and $k = 100\pi^2\,\mathrm{kg\,s^{-2}}$ so that $\epsilon_0 = 10^{-1}$ and $\ell = 101\,\mathrm{cm}$. The linear rotational mode has frequency $\omega_\mathrm{R} = \pi$ and the frequency of the elastic mode is ten times greater.

The system (4) is solved by the Bulirsch-Stoer method (Press, *et al.*, 1992, subroutine BSSTEP) which is a modern implementation of Richardson's deferred approach to the limit (Richardson and Gaunt, 1927). The slow system (12) is integrated in the same way but the diagnostic components must be solved at each step. The equation for p_r is trivial; r is deduced by an iterative procedure originally due to Picard:

$$r_0 = \ell_0(1+\epsilon_0^2\cos\theta)\,, \qquad r_{j+1} = r_0 + \frac{p_\theta^2}{kmr_j^3}\,, \tag{13}$$

which converges rapidly. The requirement to solve nonlinear diagnostic equations is characteristic of filtered systems. The numerical integration of such systems is generally more intricate than that of their unfiltered ancestors.

The initial conditions are chosen to be

$$\mathbf{X}_0 = (\theta(0), p_\theta(0), r(0), p_r(0))^{\mathrm{T}} = (-\tfrac{1}{2}, 0, \ell, 0)^{\mathrm{T}}\,.$$

These satisfy the condition of linear initialization $\mathbf{Z} = (r', p_r)^{\mathrm{T}} = \mathbf{0}$ at $t = 0$. Two integrations of (4) are performed, one from the initial conditions $\mathbf{X}_0$ and one after nonlinear initialization (10) (which yields $r(0) = r_{\mathrm{B}} \approx 1.00878$). They will be denoted respectively by LIN and NLI. They were compared to the solution of the slow system, denoted SLO. The results are presented in Fig. 4. The variation of θ with time is shown in Fig. 4(a). The rotational frequency $\omega_{\mathrm{R}} = \pi$ corresponds to one cycle every two seconds; the results are plotted for this time interval. The three graphs are so close as to be indistinguishable on the plot. The radial amplitude $\tilde{r} = -r' = \ell - r$ appears in Fig. 4(b) ($\tilde{r}$ is shown rather than r' so that the graph is low when the bob is low). The HF component is clearly visible for the linearly initialized run; note that $\omega_{\mathrm{E}} = 10\pi$ means five cycles per second. The amplitude is small—about 1.2 mm—due to the linear initialization, but still much larger than for the other runs. The NLI and SLO curves have variations with period of about one second: the nonlinear centrifugal force stretches the pendulum when the angular momentum is large; this happens twice in each rotational cycle or about once per second. These two runs are largely free from higher frequency variations but they are not coincident.

The energy (3) may be partitioned into rotational and elastic components

$$\begin{aligned} H_{\mathrm{R}} &= \frac{p_\theta^2}{2mr^2} - mgr\cos\theta + mg\ell \\ H_{\mathrm{E}} &= \frac{p_r^2}{2m} + \tfrac{1}{2}k(r-\ell_0)^2 - \tfrac{1}{2}k(\ell-\ell_0)^2\,. \end{aligned}$$

The elastic energy for the NLI and SLO integrations, together with the difference scaled by ten, is shown in Fig. 4(c). The NLI curve appears to oscillate about that of the slow run. This is confirmed by spectral analysis of the energy (Fig. 4(d)). Both runs have a major peak at one cycle per second, but the peak at five cycles per second seen for the NLI solution is not found for the SLO solution. The nonlinearly initialized solution oscillates around the manifold $\mathcal{S}_1$ with a frequency corresponding to that of the elastic waves. It must be stressed that the amplitude of these oscillations is very small—thanks to the initialization—but some oscillation is evident. A fundamental question now arises: does the complete system (4) have any solutions which are totally free from HF components, as the slow system (12) does? In other words, is there a slow manifold $\mathcal{S}$ for (12)? We investigate this in the following sections.

2.6 Singular Perturbation Expansion

The slow equations, derived above in an *ad hoc* manner can also be justified by means of more systematic scaling arguments (Lynch, 1989). We assume

as above that there is a separation of time-scales between the rotational and elastic motions, and the ratio $\epsilon = \omega_{\rm R}/\omega_{\rm E}$ is a small parameter. We first non-dimensionalize the canonical equations (4) by specifying mass and length scales m and ℓ_0 and selecting the time-scale $\omega_{\rm R}^{-1}$ of the slow rotational motion. The equations then become

$$\begin{aligned} \dot{\theta} &= p_\theta/r^2 \\ \dot{p}_\theta &= -r\sin\theta \\ \dot{r} &= p_r \\ \dot{p}_r &= -\left(\frac{r-1}{\epsilon_0^2}\right) + \left[\frac{p_\theta^2}{r^3} + \cos\theta\right] \end{aligned}$$

where all variables are now dimensionless. We next re-scale the radial variables:

$$\rho = \frac{r-1}{\epsilon_0^2}\,, \qquad p_\rho = \frac{1}{\epsilon_0} p_r\,,$$

(Georgiou and Schwartz, 1996) and the canonical equations assume the following form:

$$\begin{aligned} \dot{\theta} &= p_\theta/(1+\epsilon_0^2\rho)^2 \\ \dot{p}_\theta &= -(1+\epsilon_0^2\rho)\sin\theta \\ \epsilon_0\dot{\rho} &= p_\rho \\ \epsilon_0\dot{p}_\rho &= -\rho + \left[\frac{p_\theta^2}{(1+\epsilon_0^2\rho)^3} + \cos\theta\right]\,. \end{aligned}$$

This system is in singular perturbation form. If ϵ_0 vanishes, the radial equations reduce to algebraic relationships which determine ρ and p_ρ in terms of the angular quantities θ and p_θ. If quantities of order ϵ_0 are neglected, and the system is re-dimensionalized, the angular equations (the first pair) are

$$\dot{\theta} = p_\theta/m\ell_0^2 \qquad \dot{p}_\theta = -mg\ell_0\sin\theta$$

which govern the motion of a simple pendulum. The radial equations (the second pair) imply that the radial momentum p_r vanishes and the radius vector is given by

$$r = \ell_0\left[1 + \left(\frac{mg}{k\ell_0}\right)\cos\theta + \frac{\dot{\theta}^2}{\omega_E^2}\right]\,. \tag{14}$$

This is equivalent, up to $O(\epsilon^2)$, to the equation (10) for the manifold $\mathcal{S}_1$. The primary effect of ignoring $O(\epsilon)$ terms in the dynamical equations is the omission of the tendencies of the fast variables. This is precisely the approximation which we made above to derive the slow equations. Note that, at this order of approximation, the slow rotational motion is uninfluenced by the fast elastic motion. Colloquially, the slow motion generates a balanced fast component,

but the fast motion does not impinge upon the slow evolution. The time-scale of variations in r is the slow time-scale.

We remark that it is possible to define successively higher order balance relationships by requiring higher time derivatives of the fast variables to vanish. We can construct a hierarchy of models, the n-th-order balanced model satisfying

$$\left(\frac{d^n}{dt^n}\right) p_r = 0\,, \qquad \left(\frac{d^{n+1}}{dt^{n+1}}\right) p_r = 0$$

(Hinkelmann, 1969). The slow equations defined above are the first-order approximation in this series. The diagnostic relationships become increasingly complicated for increasing n.

3 An Outline of KAM Theory

3.1 Completely Integrable Hamiltonian Systems

Let us consider a conservative system with n degrees of freedom. The phase-space for the system is $2n$-dimensional with points specified by the canonical coordinates (q_i, p_i). Once initial conditions $(q_i(0), p_i(0))$ are given, Hamilton's canonical equations

$$\dot{q}_k = \frac{\partial H}{\partial p_k} \qquad \dot{p}_k = -\frac{\partial H}{\partial q_k} \tag{15}$$

determine the motion, which may be represented by a trajectory $(q_i(t), p_i(t))$ in phase-space. Since the system is conservative, the energy is a constant of the motion. The equation $H(q_i, p_i) = E$ specifies a $2n$–1-dimensional sub-manifold $\mathcal{E}$ called the energy manifold. Thus, the available portion of phase-space is of dimension $2n - 1$. For each additional constant of the motion which we can find, the dimensionality of the available region of phase-space is reduced by one. The key to integrating a Hamiltonian system with n degrees of freedom is to find n independent constants of motion. Suppose now that we have found n such constants, I_k (one of which is the energy). We define a canonical transformation to new coordinates, treating I_k as the new momenta, and denoting the new conjugate position coordinates as ϕ_k. One way of doing this is to define a generating function $F(q_i, I_j)$ for which the following relationships hold:

$$\phi_k = \frac{\partial F}{\partial I_k} \qquad p_k = \frac{\partial F}{\partial q_k}$$

(see, *e.g.*, Percival and Richards, 1982). Now, since the new momentum variables I_k are constant, Hamilton's equations imply

$$\dot{I}_k = -\frac{\partial H}{\partial \phi_k} = 0\,,$$

so the Hamiltonian is independent of the position coordinates ϕ_k. Furthermore, we have

$$\dot{\phi}_k = \frac{\partial H}{\partial I_k} \equiv \omega_k \quad \text{(constant)}\,,$$

so that each position coordinate $\phi_k = \omega_k t + \delta_k$ evolves linearly with time. Thus, the canonical equations are trivial to solve in this case; the system is described as *completely integrable* (we omit certain technicalities). The trajectories are confined to an n-dimensional manifold $\mathcal{M}$ of the $2n$-dimensional phase space. For bounded motion the manifold $\mathcal{M}$ may be shown to have the topology of an n-torus, that is, the cartesian product of n circles. The initial conditions determine the torus upon which the motion lies. Each torus $\mathcal{M}$ is an invariant manifold: a trajectory which starts in $\mathcal{M}$ will remain therein forever. The totality of invariant tori is said to foliate the phase space.

There is a particular system of coordinates, known as action-angle coordinates, which are especially convenient for integrable systems. It is possible to find n topologically independent closed curves $\mathcal{C}_k$ on the torus $\mathcal{M}$, none of which can be deformed into another or shrunk to a point. One defines the action variables by integrals around each of these curves:

$$I_k = \frac{1}{2\pi} \oint_{\mathcal{C}_k} \sum_{m=1}^{n} p_m \, dq_m \,. \tag{16}$$

From the generating function $F = F(q_i, I_j)$ of the associated canonical transformation one then obtains the corresponding angle variables $\phi_k = \partial F / \partial I_k$. Alternatively, they may be calculated directly from

$$\phi_k = \frac{\partial}{\partial I} \int_{(0,\cdots,0)}^{(q_1,\cdots,q_n)} \sum_{m=1}^{n} p_m \, dq_m \tag{17}$$

(Percival and Richards, 1982). Since the action variables are constant, they are determined by the initial conditions. They label the particular torus upon which the trajectory lies. The angle variables ϕ_k then give the position as a function of time.

As a concrete example, consider the harmonic oscillator with Hamiltonian $H = \frac{1}{2}(p^2/m + m\omega^2 q^2)$. The trajectories are ellipses centred at the origin. The action variable is given by

$$\begin{aligned} I = \frac{1}{2\pi} \oint p \, dq &= \frac{1}{\pi} \int_{-q_{\min}}^{-q_{\max}} \sqrt{2Em - m\omega^2 q^2} \, dq \\ &= \frac{2E}{\pi\omega} \int_{-1}^{1} \sqrt{1 - Q^2} \, dQ = \frac{2E}{\pi\omega} \int_{-\pi/2}^{\pi/2} \cos^2\theta \, d\theta = \frac{E}{\omega}\,, \end{aligned}$$

or $I = E/\omega$. Thus, the Hamiltonian is $H = H(I) = \omega I$, a function only of the new momentum coordinate I. The angle variable follows immediately, upon

expressing p in terms of q and I:

$$\begin{aligned}\phi &= \frac{\partial}{\partial I}\int_0^q p\,dq = \int_0^q \frac{\partial p}{\partial I}\,dq = \sqrt{\frac{m\omega}{2I}}\int_0^q \frac{dq}{\sqrt{1-\left(\frac{m\omega}{2I}\right)q^2}} \\ &= \int_0^{q\sqrt{2I/m\omega}} \frac{dQ}{\sqrt{1-Q^2}} = \sin^{-1}\sqrt{\frac{m\omega}{2I}}q\,.\end{aligned}$$

The original variables are then given in terms of the new ones by

$$q = \sqrt{\frac{2I}{m\omega}}\sin\phi\,, \qquad p = \sqrt{2Im\omega}\cos\phi\,. \tag{18}$$

The explicit form of the generating function $F(q,I)$ is given in Percival and Richards (*loc. cit.*, p113). The canonical equations reduce to

$$\dot{I} = -\frac{\partial H}{\partial \phi} = 0\,, \qquad \dot{\phi} = \frac{\partial H}{\partial I} = \omega\,,\ \text{constant}$$

so that the solution is immediately obvious: the action I remains constant on the trajectory and the angle variable ϕ increases linearly with time.

For $n = 2$ the tori are embedded in the 3-dimensional energy manifold $\mathcal{E}$ given by $H(I_1, I_2) = E$, and each torus divides it into inside and outside regions. Although the image is not strictly accurate, we may visualise each torus as a 2-dimensional surface in 3-dimensional euclidean space. We can define geographic coordinates ϕ_1 in the longitudinal direction and ϕ_2 in the meridional direction and take the (longest) equatorial circle as $\mathcal{C}_1$ and any meridional circle as $\mathcal{C}_2$. The trajectory on a particular torus winds around the longitudinal and meridional directions with frequencies $\omega_1 = \partial H/\partial I_1$ and $\omega_2 = \partial H/\partial I_2$. If the frequencies are rationally related (that is, if $\exists\, k, \ell \in Z$: $k\ell \neq 0, k\omega_1 + \ell\omega_2 = 0$) the motion returns eventually to its starting point and is periodic. In this situation—called the resonant case—the trajectory is a closed orbit. If the frequencies are *not* rationally related (the usual case, since the real numbers are non-denumerable) the motion never repeats itself but traces out a trajectory which is dense in $\mathcal{M}$ (it is ergodic: the time average over the trajectory equals the space average over the torus). This situation is described as quasi-periodic or conditionally periodic.

A completely integrable system is non-degenerate if the frequencies vary from one torus to another, as is usual for a nonlinear system. This is guaranteed by the following condition:

$$\mathcal{D}_1 \equiv \det\left|\frac{\partial \omega_j}{\partial I_k}\right| = \det\left|\frac{\partial^2 H}{\partial I_k \partial I_j}\right| \neq 0\,. \tag{19}$$

Then in a given energy shell some tori will have closed orbits (the resonant case of rationally related frequencies) whereas others will have quasi-periodic

orbits which never close. The set of resonant tori form a set which is dense in the energy manifold $\mathcal{E}$, but which is of measure zero (this follows from the countability of the rationals).

What happens when a completely integrable system is slightly perturbed in such a way that integrability no longer holds? Are the toroidal structures simply disturbed slightly or do they disintegrate completely? This fundamental question was answered in the early 1960s as we shall shortly see.

3.2 Canonical Perturbations and Small Divisors

Although completely integrable Hamiltonians are quite exceptional, they are important in providing a first approximation to more general systems. The most notable example is in celestial mechanics. The question of the stability of the solar system has been a concern of scientists since the time of Newton. To a first approximation the orbits of the planets are Keplerian ellipses with the Sun at a focus. These orbits are unchanging in time. However, the planets exert small attractions upon each other. It is conceivable that, over a long time, the effects of these secondary attractions may accumulate to such an extent that some of the orbits become greatly distorted. This could result in a planetary collision or in a planet crashing into the Sun or being ejected from the solar system. The Hamiltonian for the solar system may be written formally as

$$H(p_i, q_j) = H_0(p_i, q_j) + \epsilon H_1(p_i, q_j)$$

where H_0 represents the uncoupled motions of the planets governed only by the Sun, which is assumed to be stationary, and ϵH_1 accounts for all the interactions between the planets. The system is integrable for $\epsilon = 0$; the solution is completely known. In general, the planetary interactions are very small; for example, the mean force of Jupiter on Venus is less than 2×10^{-5} times that of the Sun. Thus, the solution of the full problem may be sought by means of perturbation theory.

Let us now confine attention to systems with two degrees of freedom and assume that the unperturbed motion is integrable so that, with action-angle variables, the Hamiltonian may be written in the form

$$H = H_0(I_1, I_2) + \epsilon H_1(I_1, I_2, \phi_1, \phi_2)\,. \tag{20}$$

The basic idea of canonical perturbation theory is to find a new set of action-angle variables $(J_1, J_2, \psi_1, \psi_2)$ for the perturbed system such that the Hamiltonian becomes

$$H(I_1, I_2, \phi_1, \phi_2) = K(J_1, J_2)$$

(Goldstein has suggested the name Kamiltonian for K!). If this can be done, the full system becomes completely integrable. We introduce a new generating

function $S(\phi_k, J_k)$ depending on the old angle and new action variables, such that

$$I_k = \frac{\partial S}{\partial \phi_k}; \quad \psi_k = \frac{\partial S}{\partial J_k}, \quad k = 1, 2\,.$$

Next S is expanded in a perturbation series

$$S = S_0 + \epsilon S_1 + O(\epsilon^2)$$

where the leading term $S_0 = (\phi_1 J_1 + \phi_2 J_2)$ represents the identity transformation. After some algebraic manipulation we find that

$$S_1(\phi_1, \phi_2, J_1, J_2) = \sum_k \sum_\ell \frac{H^1_{k,\ell} \exp[i(k\phi_1 + \ell\phi_2)]}{[k\omega_1 + \ell\omega_2]} \tag{21}$$

where $H^1_{k,\ell}$ are the expansion coefficients of the first order Hamiltonian and the ω's are the frequencies of the unperturbed motion: $\omega_1(I_1) = \partial H_0/\partial I_1$ and $\omega_2(I_1) = \partial H_0/\partial I_2$. A major problem now arises: if the ω's are rationally related the denominator will vanish for certain (k, ℓ); and even if the ω's are incommensurable there are values of (k, ℓ) for which $[k\omega_1 + \ell\omega_2]$ is arbitrarily small. Thus, the perturbation series cannot be shown to converge. This is the notorious *problem of small divisors*, which hampered progress in celestial mechanics for so long. The greatest mathematicians were unable to circumvent or resolve the small divisor problem and produce convergent perturbation expansions. Poincaré called it *the fundamental problem of dynamics*. The resolution came in the early 1960s with the demonstration of the celebrated Kolmogorov-Arnold-Moser or KAM theorem.

3.3 The Kolmogorov-Arnold-Moser Theorem

What the KAM theorem says, in plain language, is that *most of the original tori persist in the case of small perturbations*. They are topologically distorted but not destroyed. Thus, for most initial conditions, the trajectory remains in a manifold of dimension n and it is possible to define n action variables J_k which are constants of the motion. In this case, the motion is not qualitatively changed by a small perturbation. The exceptional cases comprise a set whose measure tends to zero with the perturbation size. The proof of the KAM theorem is long and intricate, but the key ideas are accessible and will be reviewed here.

The achievement of KAM is pivoted upon two crucial ideas. The first is to transform the perturbation series in such a way that convergence can be demonstrated under specific conditions. The result of this procedure is a series which is super-convergent. The method is to base the approximation at each stage on the best estimate available at that point, rather than on the initial

series; it is closely analogous to the iterative Newton-Raphson root-finding technique. Instead of the standard perturbation series

$$S = S_0 + \epsilon S_1 + \epsilon^2 S_2 + \epsilon^3 S_3 + \epsilon^4 S_4 + \cdots + \epsilon^n S_n + \cdots$$

one considers a series transformed in such a way that the terms decrease quadratically:

$$S = S'_0 + \epsilon S'_1 + \epsilon^2 S'_2 + \epsilon^4 S'_3 + \epsilon^8 S'_4 + \cdots + \epsilon^{2^{n-1}} S'_n + \cdots .$$

The convergence of this series for small ϵ is breath-takingly rapid. The accelerated convergence enables circumvention of the small divisor problem in most circumstances and is a cornerstone in the proof of the KAM theorem. A clear outline of the procedure is presented in Berry (1978) and Tabor (1989), and full details may be found in the original paper of Arnold (1963).

The other central idea is that one can surround each rational point on the real line by a finite interval and yet leave points uncovered by the union of all the intervals. This result is apparently paradoxical and decidedly counter-intuitive. You might argue that, since the rationals are dense on the real line, the union of a set of intervals surrounding them must be exhaustive, *i.e.*, must cover the entire real line. But you would be wrong! Consider the unit interval $[0, 1]$. Surround each rational m/n by an interval of width K/n^p. Since there are $n-1$ rationals with denominator n, the total length L of all the intervals is bounded above:

$$L \leq \sum_{n=2}^{\infty} (n-1)\frac{K}{n^p} < K \sum_{n=2}^{\infty} \frac{1}{n^{p-1}} .$$

For $p > 2$ this infinite series is convergent. If its sum is σ_{p-1}, the total length of all the intervals is less than $K\sigma_{p-1}$. Thus, provided we choose $K < 1/\sigma_{p-1}$ the total length L is less than unity, and the intervals cannot cover $[0, 1]$. If K is chosen very small, the coverage of the intervals is correspondingly meagre and the 'majority' of points are not included in their union. As $K \to 0$, the measure of the union of all the intervals which have been removed tends to zero so the residual set tends to one of full measure.

The KAM theorem shows that tori whose frequencies are rationally related are destroyed by even the smallest perturbation. Moreover, tori which are close to these resonant tori also disintegrate in the presence of a perturbation. However, this 'closeness' depends on the order of the resonance. We consider the case of two degrees of freedom (so that the $2d$-tori are embedded in a $3d$-energy manifold in $4d$-phase-space). Suppose the frequencies are such that $n\omega_1 - m\omega_2 = 0$ for some integers m and n. Then ω_1/ω_2 is rational so the torus will be destroyed. Furthermore, nearby tori whose frequency ratios are close to m/n are also destroyed; but the range of values of tori which perish decreases sharply as the denominator n increases. KAM proved convergence

of the accelerated perturbation series for all tori whose frequency ratio is sufficiently irrational for the following inequality to hold:

$$\left|\frac{\omega_1}{\omega_2} - \frac{m}{n}\right| > \frac{K(\epsilon)}{n^{2.5}}, \quad \forall\, m, n \in Z\,.$$

Here $K(\epsilon)$ is not specified precisely, but it is independent of m and n and tends to zero with ϵ. Thus, tori which do not survive the perturbation must satisfy

$$\left|\frac{\omega_1}{\omega_2} - \frac{m}{n}\right| < \frac{K(\epsilon)}{n^{2.5}}\,.$$

As we have seen, the relative measure of the union of these intervals is $K(\epsilon)\sigma_{1.5}$. As $\epsilon \to 0$ the measure of the set of destroyed tori in any bounded interval diminishes to zero. For finite ϵ the gaps resulting from low-order resonances (small n) are *relatively* wide and give rise to observable effects. The surviving tori—those not destroyed by the perturbation—comprise a set which becomes of full measure as the perturbation size vanishes. It is in this precise sense that the KAM theorem says that, for a small perturbation, most of the tori are preserved. The theorem requires ϵ to be very small indeed. The initial estimate was of the order of 10^{-48}. However, numerical experiments indicate that the qualitative character of the motion is preserved under much larger perturbations than are strictly permitted by the theorem.

The KAM theorem says nothing about the fate of the resonant tori, other than that their structure is annihilated by the perturbation. In fact, it is the destruction of these tori which is linked intimately with the genesis of chaotic behaviour. The pattern of behaviour near the rational tori which are destroyed by a perturbation is both complex and fascinating. We can describe only the essentials here; for a fuller discussion see, for example, Berry (1978), Jackson (1991), Ott (1993) or Tabor (1989). For regular motion the intersection of the torus with a plane is a closed curve. When the perturbation reaches such a size that this torus looses its integrity, the closed curve becomes a succession of alternating elliptic and hyperbolic points, the number of each being equal to the order of the resonance (the denominator of ω_1/ω_2 in the present case). The trajectories near the hyperbolic points form intricate interweaving patterns called homoclinic and heteroclinic tangles. The elliptic points form a series of regions of preserved tori—island chains—representing order in the midst of chaos. Near each elliptic point there is a repetition of this splitting of resonant trajectories on ever smaller scales, the pattern repeating itself without limit. The overall structure is a tapestry of astonishing complexity and beauty.

We now summarise the main results of the KAM theorem. For the Hamiltonian

$$H(I_i, \phi_j) = H_0(I_i) + \epsilon H_1(I_i, \phi_j)$$

the nondegeneracy condition $\mathcal{D}_1 \neq 0$ (which implies smoothly-varying frequencies) guarantees the preservation of most invariant tori under small per-

turbations ($\epsilon \ll 1$). The condition of isoenergetic nondegeneracy

$$\mathcal{D}_2 \equiv \det \begin{vmatrix} \frac{\partial^2 H}{\partial I_i \partial I_j} & \frac{\partial H}{\partial I_i} \\ \frac{\partial H}{\partial I_j} & 0 \end{vmatrix} \neq 0\,. \tag{22}$$

(which implies smoothly varying frequency *ratios*) guarantees that the total measure of the destroyed tori vanishes in the limit $\epsilon \to 0$. In an isoenergetically nondegenerate system the sets of resonant and nonresonant tori of the unperturbed system are both dense on each energy level. The former has measure approaching zero with ϵ and the latter is of full measure in this limit. The union of the tori preserved under perturbation is called the Kolmogorov set. The measure of the complement of this set does not exceed a quantity of order $\sqrt{\epsilon}$. The perturbed system is completely integrable on a Cantor set. For systems with two degrees of freedom, sharper results are available. This is because the tori partition the energy shell so that trajectories cannot cross them and chaotic orbits are sandwiched between adjacent stable tori. Subject to technical restrictions, both of the action variables remain within a distance of order ϵ from their initial values and the measure of the destroyed tori is exponentially small ($O(e^{-k/\epsilon})$). For a complete summary of results see Arnold *et al.*, 1988.

3.4 Some Consequences of the KAM Theorem

In the following sections we shall apply the KAM theory to the simple problem of the elastic pendulum. But its implications are vastly more profound. The initial impetus for the theory came from the desire to understand the stability characteristics of the solar system. There are many near-resonances; for example, the frequency ratio for Jupiter and Saturn is about 5/2, and this has a detectable effect on the orbit of Jupiter, inducing an oscillation with a period of about 900 years. While we are still far short of a complete answer to the stability problem, KAM has led to great insight into the behaviour of the planetary system. Classical perturbation theory allows us to make accurate predictions far in advance, for example, to predict solar eclipses for the next millenium. But it breaks down ultimately and tells us nothing about the stability over an indefinite time range. The power of the KAM theorem is that its conclusions are valid for unlimited time.

The theorem has enabled us to predict the stability of protons orbiting in a particle accelerator. Particles may rotate up to one trillion (10^{12}) times in the course of an experiment. Reguarding one orbit as a year, this is about the age of the Earth. Analysis by classical perturbations or by direct computation is unfeasible for such a problem but KAM theory permits the conclusion that the system is stable. The theory has also been used to explain the distribution of asteroids orbiting between Mars and Jupiter. There are clear gaps at distances

corresponding to low-order resonances with Jupiter, just where one would expect the most unstable orbits. A similar analysis has successfully accounted for the gaps in Saturn's rings. These gaps occur at locations corresponding to strong resonances with the inner satellites of Saturn. In both these cases the distribution expected from theory accords well with observations.

The KAM theorem has deep implications for statistical mechanics. Here we are concerned with macroscopic properties, such as temperature, and make no attempt to follow the details of the motion of individual components of the system. Conclusions frequently depend on the validity of the ergodic hypothesis: this assumes that the motion explores the entire region of phase space energetically available to it, ultimately covering it in a uniform way. Then time-averages can be replaced by averages over the energy level. For integrable systems only an infinitesimal portion of the energy surface is covered by the motion. It was earlier thought that the smallest perturbation of such systems would suffice to render them ergodic, but this is now known to be false. The KAM theorem implies that ergodicity does not hold in general. If time-means are to be estimated from spatial averages, the latter must be calculated over an appropriate sub-manifold of the energy shell.

4 Application of KAM to the Elastic Pendulum

4.1 Hamiltonian in Perturbation Form

We are interested in the case where there is a separation of time-scales between the rotational and elastic motions, so that the terms "slow" and "fast" make sense. In this case the ratio $\epsilon = \omega_{\mathrm{R}}/\omega_{\mathrm{E}}$ is a small parameter. The Hamiltonian may be expressed in such a form that the zeroth- and first-order problems are exactly soluble. We may then apply standard Hamiltonian perturbation theory to demonstrate some properties of the system which hold in general for small ϵ.

We first non-dimensionalise the canonical equations (4) by specifying mass and length scales m and ℓ_0 and the fast time-scale $1/\omega_{\mathrm{E}}$. The equations then become

$$\begin{aligned} \dot{\theta} &= p_\theta/r^2 && \text{(23a)} \\ \dot{p}_\theta &= -\epsilon^2 r \sin\theta && \text{(23b)} \\ \dot{r} &= p_r && \text{(23c)} \\ \dot{p}_r &= -(r-1) + p_\theta^2/r^3 + \epsilon^2 \cos\theta && \text{(23d)} \end{aligned}$$

where all variables are now dimensionless. We write $r = 1 + r'$. Assuming that the amplitude of the elastic motions is small, we introduce the scaling

$$r' = \epsilon^{1/2}\rho\,, \qquad p_r = \epsilon^{1/2} p_\rho\,,$$

so that $\rho = O(1)$ and $p_\rho = O(1)$. Then noting that $\theta = O(1)$ whereas $p_\theta = O(\epsilon)$, since we have nondimensionalised with the fast time-scale, we define $\theta = \vartheta$ and $p_\theta = \epsilon p_\vartheta$. Now the equations may be written in scaled form (with all variables $O(1)$):

$$\begin{aligned}
\dot{\vartheta} &= \epsilon p_\vartheta (1+\epsilon^{1/2}\rho)^{-2} && \text{(24a)}\\
\dot{p}_\vartheta &= -\epsilon \sin\vartheta (1+\epsilon^{1/2}\rho) && \text{(24b)}\\
\dot{\rho} &= p_\rho && \text{(24c)}\\
\dot{p}_\rho &= -\rho + \epsilon^{3/2}\left[p_\vartheta^2 (1+\epsilon^{1/2}\rho)^{-3} + \cos\vartheta\right] && \text{(24d)}
\end{aligned}$$

Using the nondimensionalisation and scaling introduced above, the nondimensional Hamiltonian may now be written as $H = \epsilon\hat{H}$, where

$$\hat{H} = \tfrac{1}{2}\left(p_\rho^2 + \rho^2\right) + \epsilon\left[\tfrac{1}{2}p_\vartheta^2(1+\epsilon^{1/2}\rho)^{-2} - (1+\epsilon^{1/2}\rho)\cos\vartheta\right] .$$

Collecting terms of equal power in ϵ this becomes

$$\begin{aligned}
\hat{H} &= H_0(\rho, p_\rho) + \epsilon H_1(\vartheta, p_\vartheta) + \epsilon^{3/2} H_2(\rho, p_\rho, \vartheta, p_\vartheta; \epsilon)\\
&= [\tfrac{1}{2}(p_\rho^2 + \rho^2)] + \epsilon[\tfrac{1}{2}p_\vartheta^2 - \cos\vartheta] + \epsilon^{3/2} H_2 .
\end{aligned}$$

The zeroth-order Hamiltonian is degenerate: it involves only the fast variables (ρ, p_ρ). The first-order perturbation removes this degeneracy without destroying integrability: the fast and slow variables are still uncoupled at this order. For the Hamiltonian $H = H_0 + \epsilon H_1$, the system is completely integrable and can be solved exactly.

4.2 Action and Angle Variables

For bounded motion of conservative Hamiltonians the analysis is greatly facilitated by the introduction of action-angle variables (Lichtenberg and Lieberman, 1992). We introduced these variables in §3.3 and considered, as an example, the coordinate transformation for a harmonic oscillator. For a one-dimensional system we defined a canonical transformation from the original conjugate variables (p, q) to the action and angle variables (I, ϕ) by

$$I = \frac{1}{2\pi}\oint p\, dq\,, \qquad \phi = \frac{\partial}{\partial I}\int_0^q p\, dq\,, \tag{25}$$

where the first integration is over a complete cycle. The Hamiltonian is then independent of ϕ and the canonical equations imply that the action I is constant ($\dot{I} = -\partial H/\partial\phi = 0$) and the angle varies linearly with time ($\omega \equiv \dot{\phi} = \partial H/\partial I$, constant). We can now specify the action-angle variables for the oscillator and pendulum. For the oscillator $H = \frac{1}{2}(p_\rho^2 + \rho^2)$ they are simply $I_\rho = H_0$ and $\phi_\rho = t$. The original variables are given by

$$\rho = \sqrt{2I_\rho}\cos\phi_\rho\,, \qquad p_\rho = \sqrt{2I_\rho}\sin\phi_\rho\,,$$

and $H_0(\rho, p_\rho) = H_0(I_\rho)$ depend only on the action variable (these results were shown in §3.1). For the pendulum ($H = \frac{1}{2}p_\vartheta^2 - \cos\vartheta$) the transformation is less trivial but is a standard problem in dynamics. As is well known, the two-dimensional phase space for the pendulum is separated into two domains by the separatrix $E = 1$ (where $E = H$ is the total energy). If $E < 1$, the motion is a *libration*, oscillating between limits $-\vartheta_{\max}$ and $\vartheta_{\max}$ where $\cos\vartheta_{\max} = -E$. For $E > 1$, the motion is *rotational* with the pendulum revolving completely around its point of suspension.

We assume here that the motion is libratory. The period of oscillation is given by

$$T = 2\int_{-\vartheta_{\max}}^{\vartheta_{\max}} \frac{d\vartheta}{[2(E+\cos\vartheta)]^{1/2}} .$$

As $\vartheta_{\max} \to \pi/2$ the period tends to infinity. The action-angle variables are different for each regime; for libratory motion they are

$$I_\vartheta(E) = \frac{2}{\pi}\int_0^{\vartheta_{\max}} [2(E+\cos\vartheta)]^{1/2}\, d\vartheta$$

$$\phi_\vartheta(E,\vartheta) = \left(\frac{dI}{dE}\right)^{-1} \int_0^{\vartheta} \frac{d\vartheta}{[2(E+\cos\vartheta)]^{1/2}}$$

These may be transformed into standard elliptic integrals (see Lichtenberg and Lieberman, 1992 for fuller details and for the rotatory case).

The Hamiltonian of the elastic pendulum may now be written in terms of the action-angle variables:

$$\hat{H} = H_0(I_\rho) + \epsilon H_1(I_\vartheta) + \epsilon^{3/2} H_2(I_\rho, \phi_\rho, I_\vartheta, \phi_\vartheta; \epsilon) . \tag{26}$$

The first two terms describe uncoupled motion of the oscillator and pendulum. This system is integrable: both H_0 and H_1 are constants, their values being determined by the initial conditions. The Hamiltonian

$$H_{\text{unc}} = H_0(I_\rho) + \epsilon H_1(I_\vartheta) \tag{27}$$

is independent of the angle variables. The motion for given actions I_ρ and I_ϑ is described by a trajectory lying in a torus $\mathcal{T}$ which is the product of closed curves:

$$\mathcal{T}(I_\rho, I_\vartheta) = \{(I_\rho, \phi_\rho) : 0 \le \phi_\rho \le 2\pi\} \times \{(I_\vartheta, \phi_\vartheta) : 0 \le \phi_\vartheta \le 2\pi\} .$$

The trajectories may densely cover the torus with the angle variables running around the two directions of the surface (this is the typical case); or, in the exceptional case of commensurate frequencies (when the quotient of the frequencies is rational), they may form closed curves winding around each direction an integral number of times. The exceptional case is referred to as resonance.

The total Hamiltonian is a perturbation of this system, and may be described as near-integrable. In the case of two degrees of freedom the generic character of the motion for such systems is well understood. The trajectory lies on a three-dimensional constant energy surface $\mathcal{E}$ embedded in the four-dimensional phase space. There are regions of regular motion and regions of stochasticity or chaos. The two species of solution are closely intermingled, with regular trajectories separating chaotic regions. (For more degrees of freedom the regular trajectories no longer separate the chaotic regions, which are connected in a single complex structure called the Arnold web).

4.3 Implications of the KAM Theorem

We wish to apply the results of the Kolmogorov-Arnold-Moser theorem, as presented in §3.3 above, to the problem of the elastic pendulum. The discussion in this section owes much to the work of Bokhove and Shepherd, 1996 (BS96), who discussed the behaviour, for small values of the coupling parameter ϵ, of the Lorenz model. The relationship between the Hamiltonian for the elastic pendulum and the system studied in BS96 is indicated by the following relationships (their notation on *rhs*):

$$\vartheta = 2q_1\,, \quad p_\vartheta = 2p_1\,, \quad \rho = q_2\,, \quad p_\rho = p_2\,,$$

with $4\epsilon = \varepsilon$ and parameter values $C = \frac{1}{2}$ and $b = \frac{1}{2}$. Then the Hamiltonian becomes

$$\hat{H} = H_0(q_2, p_2) + \varepsilon H_1(q_1, p_1) + \varepsilon^{3/2} H_2(q_1, p_1, q_2, p_2; \varepsilon)\,,$$

with $H_0 = \frac{1}{2}(p_2^2 + q_2^2)$ and $H_1 = \frac{1}{2}(p_1^2 - C\cos 2q_1)$, which is identical to order ϵ with (13) in BS96. Of course, the coupling terms, embodied in the function H_2, are not identical for their model and for the elastic pendulum, but the precise details of these terms do not affect the general character of the solutions for small ϵ. We therefore find that the conclusions of Bokhove and Shepherd are also valid in the present case.

A condition for applicability of the KAM result is that the first-order or uncoupled Hamiltonian $H_{\rm unc} = H_0 + \epsilon H_1$ be isoenergetically nondegenerate (Arnold, 1978). Recall that this requires the nonvanishing of the determinant $\mathcal{D}_2$. In the present case we obtain

$$\mathcal{D}_2 \equiv \begin{vmatrix} \frac{\partial^2 H_{\rm unc}}{\partial I_\rho^2} & \frac{\partial^2 H_{\rm unc}}{\partial I_\rho \partial I_\vartheta} & \frac{\partial H_{\rm unc}}{\partial I_\rho} \\ \frac{\partial^2 H_{\rm unc}}{\partial I_\vartheta \partial I_\rho} & \frac{\partial^2 H_{\rm unc}}{\partial I_\vartheta^2} & \frac{\partial H_{\rm unc}}{\partial I_\vartheta} \\ \frac{\partial H_{\rm unc}}{\partial I_\rho} & \frac{\partial H_{\rm unc}}{\partial I_\vartheta} & 0 \end{vmatrix} = \begin{vmatrix} \frac{\partial \omega_\rho}{\partial I_\rho} & \frac{\partial \omega_\vartheta}{\partial I_\rho} & \omega_\rho \\ \frac{\partial \omega_\rho}{\partial I_\vartheta} & \frac{\partial \omega_\vartheta}{\partial I_\vartheta} & \omega_\vartheta \\ \omega_\rho & \omega_\vartheta & 0 \end{vmatrix} = \begin{vmatrix} 0 & 0 & \omega_\rho \\ 0 & \frac{\partial \omega_\vartheta}{\partial I_\vartheta} & \omega_\vartheta \\ \omega_\rho & \omega_\vartheta & 0 \end{vmatrix}$$

(we have written $\omega_\rho \equiv \omega_{\rm E}$ and $\omega_\vartheta \equiv \omega_{\rm R}$ for the unperturbed fast and slow frequencies, respectively). The condition requires that the frequency ratio

$\omega_{\rm R}/\omega_{\rm E}$ varies from torus to torus. This is so in the present case because, although $\omega_{\rm E}$ is constant, the frequency of the (nonlinear) pendulum varies with the action variable, so we have $\mathcal{D}_2 = -\omega_\rho^2\,\partial\omega_\vartheta/\partial I_\vartheta \neq 0$. At the separatrix of the pendulum, when the period tends to infinity and the frequency to zero, the condition fails.

Provided we avoid the separatrix, the conclusions of the KAM theorem (Arnold, *et al.*, 1988) are applicable in the present case. For small ϵ most of phase-space is filled by invariant tori that are smooth deformations of the invariant tori $\mathcal{T}(I_\rho, I_\vartheta)$ of the uncoupled system. Most of the original tori persist for a small enough perturbation and the solution remains regular on these tori. They are dense in $\mathcal{E}$ — the measure of the complement of their union vanishes as $\epsilon \to 0$ — and they tend smoothly to the unperturbed tori which foliate the corresponding level surface of $\mathcal{E}$ in this limit. There are thin regions of chaotic motion around resonant tori. However, the theory ensures that the measure of these regions tends to zero exponentially fast—like $e^{-k/\epsilon}$—as $\epsilon \to 0$. The preserved two-dimensional tori partition the three-dimensional accessible portion of phase space and trajectories cannot cross them. Thus, chaotic orbits are tightly confined between adjacent regular tori.

In terms of slow mode–fast mode interactions (analogous to Rossby wave–gravity wave interactions in the atmosphere), this result means that if most of the energy is initially in the slow mode, *i.e.*, if the starting state is initialized, only an amount proportional to the coupling constant ϵ can be transferred to the fast oscillations. It would be gratifying if we could draw the following conclusion for the Rossby wave–gravity wave interactions in the real atmosphere: *if most of the energy is initially in the Rossby waves,* i.e.*, if the starting state is initialized, only an amount proportional to the coupling constant ϵ can be transferred to the gravity waves.* Unfortunately, such a conclusion is unjustified: it must be stressed that the above result is rigorously valid only for a model with two spatial dimensions. In higher dimensional phase spaces the tori do not isolate the surfaces of constant energy and transfer of energy between modes by the process of Arnold diffusion is possible. However, this process is very weak and occurs over a long time scale, so that, in practice, the statement italicised above may indeed be valid.

5 Numerical Investigation of Regular and Chaotic Motions

5.1 Poincaré Sections

To gain further insight into the nature of the motion for small ϵ, a series of numerical integrations of the canonical equations were performed. The results will be presented in this section. The trajectories are one-dimensional curves on a three-dimensional energy manifold in four-dimensional phase space. The

best means of depicting such curves on paper is not immediately obvious. However, Poincaré proposed a simple method which is particularly attractive for autonomous systems with two degrees of freedom. To visualise the motion, we choose a two-dimensional surface and plot the intersection of a trajectory each time it passes through the surface in a particular direction. The result is called a Poincaré section. Two especially convenient choices are the 'slow' or (ϑ, p_ϑ) plane with $\rho = 0, p_\rho > 0$ and the 'fast' or (ρ, p_ρ) plane with $\vartheta = 0, p_\vartheta > 0$. The distribution of points on the section can reveal whether or not the motion is integrable. If it is, the trajectory lies on a torus which cuts the section in a smooth curve. For non-integrable motion the system explores a three-dimensional region of the energy level, whose intersection with a plane is an area rather than a curve. Thus, for regular motion the set of trajectory intersections lies on a closed invariant curve, covering it densely. In the exceptional case of rational ratio of frequencies the section comprises a finite number of points. For chaotic motion the representative points fill a finite area of the section. We recall that strict applicability of the KAM theorem requires that the perturbation parameter ϵ be extremely small (typically about $O(10^{-48})$). This is far below the range of practical interest. Thus, numerical experimentation is required to investigate the solutions for more reasonable values of ϵ. Although the KAM results may not apply for such values, it is found that Poincaré sections interpreted in the spirit of the KAM theorem can be very illuminating and instructive.

5.2 Numerical Solutions

Numerical integrations of the canonical equations have been carried out using a modified explicit symplectic integrator (Yoshida, 1990). It was found convenient to rescale the system (24) using the slow time-scale ω_{R}^{-1}. The Yoshida scheme is applicable for Hamiltonians of the form

$$H(\mathbf{p}, \mathbf{q}) = T(\mathbf{p}) + V(\mathbf{q}) \,.$$

As the Hamiltonian for the elastic pendulum is not of this form, a modification of the scheme was required. It was possible to preserve second-order accuracy for the modified scheme (Onno Bokhove, personal communication). The scheme executes each forward time step as a canonical transformation, preserving phase space volume elements. The total energy is also conserved to very high accuracy: for a time step $\Delta t = 0.0001$, the energy varied by less than ten parts per million.

The rescaled equations (24) were solved for two values of the total energy, $E = 0$ and $E = 1.8$. For each energy, some twelve different choices of initial conditions were used, each choice partitioning the energy differently between rotational and elastic components. For each total energy, the equations were integrated for an increasing set of values of ϵ, six in all:

$\epsilon \in \{0.025, 0.05, 0.1, 0.25, 0.325, 0.4\}$. For smaller perturbation values ($\epsilon \ll 1$) the coupling is weak and we expect behaviour similar to that of the uncoupled system. For the largest values the separation of time scales is no longer clear-cut, the coupling is strong and we must expect the interaction between the rotational and elastic components to be significant.

The results for the two choices of energy are shown in Fig. 6 ($E = 0$) and Fig. 7 ($E = 1.8$). For each set of integrations (each fixed E and ϵ) two sections are shown, the section in the slow variables (ϑ, p_ϑ) above and the section in the fast variables (ρ, p_ρ) below. Each trajectory leaves a signature in both planes. Since E is fixed, the high energy orbits in the slow plane must correspond to the low energy ones in the fast plane, and vice versa.

We consider first the low energy case $E = 0$. For this value of E, the trajectories are within the separatrix for all partitions between rotational and elastic energy. The three panels in the top row of Fig. 6 show the slow-plane section for the three low values of ϵ. The panels in the second row are the corresponding sections in the fast plane. The slow sections are similar to those of a simple pendulum in libratory motion (Fig. 5). The fast section curves resemble the elliptic trajectories of a harmonic oscillator. The central point represents a solution for which there is no high frequency activity. As ϵ increases, this 'core' point moves from the origin along the positive ρ-axis. This is in accordance with our discussion of nonlinear initialization, where we found that the solution is expected to have minimal high frequency activity when $(r, p_r) = (r_\mathrm{B}, 0)$. Recall from (14) that $r_\mathrm{B} = \ell(1 + O(\epsilon^2))$ so that $\rho = O(\epsilon^{3/2})$ and the core point should move away from the origin of the fast plane as ϵ increases. For the core solution we see that $p_\rho \approx 0$, in agreement with §2.3.

For the small values of ϵ the phase portraits are very similar to those of a simple pendulum (panels *a–c*) and a harmonic oscillator (panels *d–f*). As ϵ increases—panels *g–l* of Fig. 6 are for $\epsilon \in \{0.25, 0.325, 0.4\}$—some of the toroidal structures are seen to disintegrate into chaotic regions. For $\epsilon = 0.25$ a fourth-order resonance is clear (panel *g*, third row). For $\epsilon = 0.325$ (panel *h*) a third-order resonance is seen nearer the centre. When $\epsilon = 0.4$ the solution begins to appear chaotic, with the points appearing to fill an area near the centre. Complex patterns of island chains are evident in the section (panel *i*, third row). For higher rotational—and lower elastic—energy, the motion still appears to be regular at this perturbation level.

When $E = 1.8$ and the elastic energy is small, the motion of the pendulum is rotatory, lying entirely outside the separatrix (see Fig. 7). If relatively more energy resides in the elastic oscillation, the pendulum motion is libratory (within the separatrix). For some initial conditions the solution is close to the separatrix; this is the situation in which we may expect chaotic behaviour to first become evident as ϵ increases. For small ϵ (first two rows, Fig. 7) the solution is again close to the uncoupled solution. By $\epsilon = 0.25$ we see the beginning of chaotic motion near the separatrix (panel *g*, third row) together

with a fourth-order resonance. For larger ϵ the dynamics are predominantly chaotic; the regions of regular motion are relatively small. A correspondence can be made between regions of regular motion in the fast and slow planes; and also between the chaotic regimes in the two planes.

5.3 Existence of the Slow Manifold

The existence of a slow manifold is intimately related to the following question: given an initial state $(I_\vartheta(0), \phi_\vartheta(0), I_\rho(0), \phi_\rho(0))$, can we modify the fast variables $(I_\rho(0), \phi_\rho(0))$ in such a way that fast oscillations are absent from the solution for all time? In the uncoupled case, we eliminate all fast oscillations by setting the initial fast action $I_\rho(0)$ to zero. This corresponds to linear initialization and ensures that the fast action remains zero in perpetuity. In this special case, the torus is replaced by a simple closed curve. We call this the core solution (following Bokhove and Shepherd, 1996). The Poincaré section in the fast plane then collapses to a single point at the origin. The question now is: for non-zero perturbation ϵ, can we define new action-angle variables (J_ρ, ψ_ρ) such that there is a core solution with $J_\rho = 0$? If so, the fast variations can be eliminated. The KAM theorem guarantees that for most initial conditions (the exceptional cases being of measure zero) the toroidal topology of the uncoupled solution is preserved for sufficiently small perturbations. We can find toroidal sections arbitrarily close to the core solution ($I_\rho = 0$) in the fast plane whose structure is preserved for small ϵ. For non-zero ϵ the core point is no longer at the origin—the fast variables are not identically zero—but the trajectory still reduces to a single point in the fast plane. Thus, there is no high frequency variability in the solution. (Strictly, it must be confirmed that this is still true after transformation back to the original variables; see BS96). This situation corresponds to a nonlinear initialization which ensures complete absence of free high frequency motions for all time. Unfortunately, although the KAM theorem assures us of the existence of such initial values, it gives us no inkling of how to find them, and alternative methods must be used (see, *e.g.*, Lorenz, 1986). Most initialization schemes control high frequency noise but do not remove it entirely.

The numerical results presented above increase our confidence that a core solution exists for small ϵ. Looking at Figs. 6–7, we can see that evidence of trajectories whose fingerprint in the fast plane is just a single point. As ϵ increases it becomes more difficult to unequivocally identify a core solution. Thus, it seems there is a perturbation size beyond which it is no longer possible to define initial conditions which guarantee regular, slow evolution.

In summary, for small ϵ there is a slow manifold, a sub-manifold of phase space which is invariant and devoid of free high frequency oscillations. It is not simply connected but has a complex topology, being perforated by exceptional points corresponding to breakup of invariant tori near resonances (BS96). However, the exceptional points amount to a set of exponentially

small measure. For large ϵ the distinction between slow and fast motion becomes unclear, the coupling becomes strong and it is no longer possible to define initial conditions which guarantee absence of 'fast' variations.

6 Resonance of the Elastic Pendulum

In general, the coupling between the elastic and rotational motions of the pendulum is weak and undramatic. There is a special case in which this is not so: when the frequency of the elastic oscillations is approximately twice that of the rotational motion, an extraordinary interaction occurs, in which energy is transferred back and forth periodically between the two kinds of motion. Indeed, it is fascinating to watch the behaviour of a physical pendulum oscillating in this way. The dynamics of this nonlinear resonance phenomenon will be discussed in this section.

6.1 Parametric Resonance

The solution of a linear system which has a sinusoidal character for constant parameter values can grow exponentially if a parameter varies periodically with time. This phenomenon is called parametric resonance (Landau and Lifshitz, 1969; Minorsky, 1962). It can be demonstrated easily by holding the string of a pendulum lightly in the fingers of one hand while pulling with the other as it passes through the vertical and releasing as it reaches the extremities. A more dramatic example of the phenomenon is the incense burner in Santiago de Compostella (Berry, 1978). Perhaps the simplest and best known example occurs when a child alternately stands and squats on a swing. If the centre of mass is thus raised and lowered with a period twice the natural period, a swinging motion of growing amplitude can be induced (Curry, 1976).

We consider a pendulum with periodically varying length. We assume the string remains taut throughout the motion. The Lagrangian for the angular motion of the system may be written as:

$$L = T - V = \tfrac{1}{2} m r^2 \dot{\theta}^2 + mgr\cos\theta$$

where the length $r = r(t)$ is prescribed. The equation for the pendular motion is

$$\ddot{\theta} + \frac{2\dot{r}\dot{\theta}}{r} + \frac{g}{r}\sin\theta = 0\,.$$

If we define $\vartheta = r\theta/\ell$, the equation becomes

$$\ddot{\vartheta} + \frac{g}{\ell}\sin\left(\frac{\ell\vartheta}{r}\right) - \frac{\ddot{r}}{r}\vartheta = 0\,.$$

We now assume the length varies sinusoidally with frequency Ω:

$$r = \ell(1 + \eta \cos \Omega t) \, .$$

Moreover, we assume that η and ϑ are small. Then the equation may be written

$$\ddot{\vartheta} + \left[\omega^2 - \eta(\omega^2 - \Omega^2) \cos \Omega t\right] \vartheta = 0 \, , \tag{28}$$

where $\omega = \sqrt{g/\ell}$ is the frequency for the unperturbed case ($\eta = 0$). This may be expressed as Mathieu's equation in the canonical form

$$\frac{d^2\vartheta}{d\tau^2} + [a - 2q \cos 2\tau] \, \vartheta = 0 \, , \tag{29}$$

where the quantities τ, a and q are defined as follows:

$$\tau = \tfrac{1}{2}\Omega t \qquad a = \left(\frac{2\omega}{\Omega}\right)^2 \qquad q = 2\eta \left(\frac{\omega^2}{\Omega^2} - 1\right) \, .$$

Growing solutions of Mathieu's equation are known to exist for certain parameter values. We can see this heuristically by treating the small term in (28) as a forcing term:

$$\ddot{\vartheta} + \omega^2 \vartheta = \tfrac{1}{2} q \Omega^2 (\cos \Omega t) \vartheta \, .$$

For $q = 0$ the solution is $\vartheta = A \cos(\omega t - \psi)$. Substituting this, the right-hand side becomes

$$\tfrac{1}{4} A q \Omega^2 \Big\{ \cos[(\Omega + \omega)t - \psi] + \cos[(\Omega - \omega)t - \psi] \Big\} \, .$$

Clearly, this acts as a resonant forcing if $(\Omega - \omega) = \omega$ or $\Omega = 2\omega$. Thus, if the parametric variation is at twice the 'natural' frequency ω, a growing solution may be expected; this is parametric resonance.

The solutions of Mathieu's equation have been studied intensively; the standard reference is McLachlan (1947). The general theory of equations with periodic coefficients is called Floquet theory. They have solutions of the form $\exp(\gamma t)\phi(t)$, where γ is real or complex depending on the values of the parameters and ϕ is periodic, with period π or 2π. Thus, the character of the solutions of Mathieu's equation depends strongly on the values of the parameters. The a–q-plane is divided by transition curves into stable and unstable regions. In the former, the solutions remain bounded for large τ. In the latter, one of the solutions grows exponentially. On the transition curves the solutions are periodic.

Nayfeh (1973) applied several perturbation techniques to derive approximate expressions for the transition curves. For small values of q, the solutions are stable except for thin regions near where a is a perfect square. The widest region and the fastest rate of exponential growth occur for the case $a = 1$,

corresponding to $\Omega = 2\omega$. Thus, if the length of the pendulum is varied with small amplitude at a frequency twice the natural frequency of oscillation, the amplitude of the swinging motion can grow exponentially. As the amplitude increases, the approximations made are violated, the characteristic period increases and resonance no longer obtains. Thus, the system equilibrates at a finite amplitude.

Parametric resonance has important consequences in plasma physics, solid-state physics, nonlinear optics and electronics. We have mentioned the quantum phenomenon of Fermi resonance found, for example, in the infra-red spectrum of CO_2. The elastic pendulum provides a classical analogue for this; indeed, it was this problem which prompted the Russian physicist Mandlestam to propose the study of the simple mechanical system to Vitt and Gorelik (1933). Parametric resonance is relevant for the stability of orbits in particle accelerators. It can also result in catastrophic instability of mechanical systems. For example, it has long been known that a ship for which the natural frequencies for heave and roll are in the ratio 2:1 can have undesirable dynamical characteristics. Paulling and Rosenberg (1959) have applied the concept of parametric resonance to analyse unstable ship motions resulting from nonlinear coupling. The instability was confirmed by construction and testing of a model. Their analysis highlights the inadequacy of linear stability analysis in ship design.

6.2 The Small Amplitude Approximation

We now study small amplitude solutions, keeping only linear and quadratic terms in the equations of motion. We can approximate the equations directly, but it is more convenient to expand the potential energy, keeping terms to cubic order. We employ cartesian coordinates with horizontal and vertical axes x and z originating at the point of equilibrium of the pendulum. For small amplitudes, these coordinates yield equations equivalent to but less clumsy than the apparently more natural polar coordinates which we have used above. The kinetic and potential energies are

$$T = \tfrac{1}{2}m(\dot{x}^2 + \dot{z}^2)\,, \qquad V = \tfrac{1}{2}k(r - \ell_0)^2 + mgz\,,$$

where $r^2 = x^2 + (z - \ell)^2$ is the instantaneous length of the pendulum (Davidović et al., 1996). The equations of motion can be written immediately:

$$\ddot{x} + \omega_{\rm E}^2(r - \ell_0)\frac{x}{r} = 0 \tag{30}$$

$$\ddot{z} + \omega_{\rm E}^2(r - \ell_0)\frac{z}{r} + g = 0\,. \tag{31}$$

We can simplify considerably in the case of small amplitude motion. Expanding r to cubic order we find that

$$r = \ell\left[1 - \frac{z}{\ell} + \frac{x^2}{2\ell^2} + \frac{x^2 z}{2\ell^3}\right]\,.$$

This is substituted into the potential energy function to obtain, to third order,

$$V = \tfrac{1}{2}m\left[\omega_{\mathrm{R}}^2 x^2 + \omega_{\mathrm{E}}^2 z^2 - \lambda x^2 z\right] + V_0$$

where $\lambda = (\omega_{\mathrm{E}}^2 - \omega_{\mathrm{R}}^2)/\ell = \omega_{\mathrm{E}}^2 \ell_0/\ell^2$ and V_0 is a constant. If quadratic terms only are retained, the equi-potential lines are ellipses, corresponding to two decoupled harmonic oscillators. The cubic term distorts them into banana-shaped curves (see Fig. 8). The equations of motion now become

$$\ddot{x} + \omega_{\mathrm{R}}^2 x = \lambda x z \tag{32}$$
$$\ddot{z} + \omega_{\mathrm{E}}^2 z = \tfrac{1}{2}\lambda x^2 . \tag{33}$$

Omitting the small right-hand terms, the horizontal and vertical motions are

$$x = A\cos(\omega_{\mathrm{R}} t - \psi) \qquad z = B\cos(\omega_{\mathrm{E}} t - \chi) .$$

In the special case $\omega_{\mathrm{E}} = 2\omega_{\mathrm{R}}$, the effect of the quadratic terms is profound. We shall examine this in more detail. First, consider the case where the spring mode of oscillation is dominant, $|x| \ll |z|$. The vertical motion is given approximately by $z = B\cos(\omega_{\mathrm{E}} t - \chi)$. Then the x-equation is

$$\ddot{x} + [\omega_{\mathrm{R}}^2 - \lambda B\cos(\omega_{\mathrm{E}} t - \chi)]x = 0 .$$

Defining $\tau = \frac{1}{2}(\omega_{\mathrm{E}} t - \chi)$, $a = (2\omega_{\mathrm{R}}/\omega_{\mathrm{E}})^2 = 4\epsilon^2$ and $q = 2\ell_0 B/\ell^2 = 2(1 - \epsilon^2)B/\ell$, we get

$$\frac{d^2x}{d\tau^2} + [a - 2q\cos 2\tau]x = 0 .$$

This is Mathieu's equation and we know from the discussion on parametric resonance that there is an unstable region near $a = 1$ or $\omega_{\mathrm{E}} = 2\omega_{\mathrm{R}}$. Thus, a vertical motion will induce an exponentially growing horizontal motion if the ratio of the frequencies is two-to-one.

Next we assume that the pendulum mode is dominant ($|x| \gg |z|$) and consider the vertical equation. The horizontal motion is given approximately by $x = A\cos(\omega_{\mathrm{R}} t - \psi)$ so the z-equation may be written

$$\ddot{z} + \omega_{\mathrm{E}}^2 z = \tfrac{1}{4}\lambda A^2\left[1 + \cos 2(\omega_{\mathrm{R}} t - \psi)\right] .$$

The first right-hand term induces a constant deflection. The second gives rise in general to a response at the forcing frequency $2\omega_{\mathrm{R}}$. But if this corresponds to the natural frequency, i.e., if $2\omega_{\mathrm{R}} = \omega_{\mathrm{E}}$, there is resonance and the z-solution grows linearly with time.

In summary, in the resonant case—where the frequency of the spring motion is twice that of the pendular motion—a vertical oscillation of the pendulum will induce a horizontal one, and *vice versa*.

6.3 General Analysis of Resonance

In the resonant case there is a periodic exchange of energy between the two modes of oscillation, a slow recurrence or vacillation. This cannot be seen from the above simple discussion but requires a deeper examination. Perturbation analyses have been carried out using a variety of techniques. The first fairly complete analysis was by Vitt and Gorelik (1933), who deduced expressions for the slowly-varying amplitudes and for the period of recurrence in terms of elliptic functions and integrals. Van der Burgh (1968) applied the method of averaging, obtaining similar results. Kane and Kahn (1968) performed a perturbation analysis of the Hamilton-Jacobi equation, confirming their results by numerical integrations. Nayfeh (1973) examined the problem from several viewpoints, deriving equations for the slowly-varying terms but not discussing their consequences. Breitenberger and Mueller (1981) analysed the system using the slow-fluctuation approximation, which is similar to the averaged Lagrangian technique. Cayton (1977), Rusbridge (1980) and Lai (1984) applied the stroboscopic method of Minorsky (1962). Falk (1978) carried out a multiple time-scale analysis, but his paper contains a serious error, as pointed out by Lai (1984), and the results are wrong.

We shall not present a full perturbation analysis here but shall state some of the principal results (the discussion below is based mainly on Lai, 1984). Let us seek a solution of (32)–(33) in the form

$$x = A(t)\cos(\omega_{\mathrm{R}} t + \psi(t))\,, \qquad z = B(t)\cos(\omega_{\mathrm{E}} t + \chi(t))\,,$$

where the amplitudes $A(t), b(t)$ and phases $\psi(t), \chi(t)$ are presumed to be slowly varying. By means of a multiple time-scale analysis (or other perturbation technique), we may derive a system of equations for the slow variables:

$$\begin{aligned}
\dot{A} &= -\kappa AB\sin(2\psi-\chi) && (34)\\
\dot{B} &= +\tfrac{1}{4}\kappa A^2\sin(2\psi-\chi) && (35)\\
\dot{\psi} &= -\kappa B\cos(2\psi-\chi) && (36)\\
\dot{\chi} &= -\tfrac{1}{4}\kappa(A^2/B)\cos(2\psi-\chi) && (37)
\end{aligned}$$

where $\kappa = 3\omega_{\mathrm{R}}/4\ell$ is a constant. The phase equations may be combined into a single equation for $\gamma = 2\psi - \chi$:

$$\dot{\gamma} = -\kappa\left(2B - \frac{A^2}{4B}\right)\cos\gamma\,.$$

Eliminating γ from the amplitude equations we derive a constant of the motion:

$$A^2 + 4B^2 = M_0^2\,.$$

This is a consequence of conservation of energy. Next, multiplying the phase equation by $\tan\gamma$ and using the amplitude equations, we deduce a second

constant:

$$A^2 B \cos\gamma = N_0 \,.$$

Since there are two independent constants of the motion, the system is completely integrable (but recall that this depends on various small amplitude approximations). We may deduce a single equation for $\alpha = A^2/M_0^2$:

$$\frac{d^2\alpha}{dt^2} + \left(\tfrac{3}{2}\kappa M_0^2\right)\alpha(\alpha - \tfrac{2}{3}) = 0\,, \tag{38}$$

and the solution may be expressed in terms of a Jacobian elliptic function. The period of the elliptic function is the period of vacillation of energy; it depends strongly on the amplitude of the motion.

We note that the above perturbation analysis is valid only for small amplitudes. Núñez-Yépez, *et al.* (1990) have shown in a numerical study that the system goes from regular to chaotic and back to regular behaviour as the total energy is increased.

We illustrate the vacillating solution by a simple example. The parameter values are $m = 1$, $g = \pi^2$, $k = 4\pi^2$ and $\ell = 1$ (all SI units), so that $\epsilon = 0.5$ and the periods of the swinging and springing motions are respectively $\tau_{\rm R} = 2$s and $\tau_{\rm E} = 1$s. The initial conditions are vanishing velocity ($\dot{x} = \dot{z} = 0$), with $x(0) = 0.005$ and $z(0) \in \{0.05, 0.1\}$ (over 99% of the energy is initially in the elastic component). The exact equations are integrated over a period of 140 seconds, and the amplitudes of the horizontal and vertical components of motion are shown in Fig. 9. The slow vacillation of energy back and forth between springy and swingy motion is clear. Fig. 9(a) is for the smaller energy, $z(0) = 0.05$ and has a vacillation period of about 70s. Fig. 9(b), for the larger energy ($z(0) = 0.1$), has a significantly faster vacillation, the period now being about 40s. The envelop of the amplitudes may be closely approximated by elliptic functions. The total energy was checked during the integrations, and found to be constant to within 0.001%.

A physical spring pendulum, not constrained to a single plane, shows an interesting effect: when started with predominantly vertical motion, it moves in different vertical planes during successive horizontal excursions, in an apparently random fashion. The pattern of motion appears to be highly sensitive to the initial conditions, and essentially unpredictable. Thus, while the period of vacillation is highly regular, its direction would seem to be completely chaotic. This phenomenon merits further investigation.

7 Concluding Discussion

7.1 Complementary Studies

The pendulum has a hyperbolic (saddle-point) equilibrium at $\theta = \pm\pi$, connected to itself by a pair of homoclinic orbits which form the separatrix. The

numerical results presented in §5 suggested an early onset of chaotic motion there: the Poincaré sections had the appearance of irregularity near the separatrix for relatively small ϵ (see, *e.g.*, Fig. 7*g*). The system is isoenergetically degenerate as well as degenerate and the KAM theorem is inapplicable on the separatrix. Alternative methods must be used for the theoretical study of the solution in this region. Holmes and Marsden (1982) investigated the dynamics of a coupled pendulum-oscillator system using the Melnikov function technique. They assumed a perturbation term in the Hamiltonian of the form $H'(\rho, p_\rho) = \frac{1}{2}\epsilon(\rho - \theta)^2$ which corresponds to linear coupling in the canonical equations:

$$\dot{\theta} = p_\theta\,, \qquad \dot{p}_\theta = -\sin\theta + \epsilon(\rho - \theta)\,,$$
$$\dot{\rho} = p_\rho\,, \qquad \dot{p}_\rho = -\omega^2\rho - \epsilon(\rho - \theta)\,.$$

They showed that for initial conditions sufficiently near the separatrix this system has Smale horseshoes in its dynamics and consequently possesses no analytic second integral. The horseshoes are generated by the tangling of the stable and unstable manifolds of trajectories homoclinic to $\theta = \pm\pi$. The existence of a horseshoe map on the energy surface implies sensitivity to initial conditions and the presence of chaotic dynamics. The same technique could be applied to the elastic pendulum (although we should not anticipate the outcome before the analysis is performed).

Camassa (1995) studied the dynamics of the Lorenz (1986) system near the saddle-point equilibrium $P_{\rm H}$ using a combination of Melnikov and singular perturbation methods. He showed the existence of a countable infinity of homoclinic bifurcations near $P_{\rm H}$ and demonstrated the chaotic nature of the dynamics in the vicinity of the separatrix. Camassa pointed out (*loc. cit.*, p317) that some of his analysis can be applied to the generic situation of a Hamiltonian with a saddle-point equilibrium. To the extent that this claim is valid, his conclusions for the Lorenz system could also be applicable to the elastic pendulum. Camassa and Tin (1996) extended this study to the forced and damped version of the Lorenz model. They concluded that a local slow manifold exists near the hyperbolic point. This conclusion also held true for the conservative case. But a global slow manifold, defined *either* as an invariant manifold devoid of fast oscillations for all time *or* as an invariant manifold for which the fast variables are functions of the slow ones (*i.e.*, slaved to them), does not exist.

7.2 Centre Manifold Theory

The Lyapunov subcentre manifold theorem (Kelley, 1967) provides useful information about the character of the dynamics in the vicinity of the equilibrium points. The theorem applies to a system of the form

$$\dot{p} \;=\; \lambda q + P(p, q, \mathbf{r})$$

$$\begin{aligned} \dot{q} &= -\lambda p + Q(p, q, \mathbf{r}) \\ \dot{\mathbf{r}} &= \mathbf{A}\mathbf{r} + \mathbf{R}(p, q, \mathbf{r}) \end{aligned}$$

where p and q are two scalars and $\mathbf{r}$ is a vector of the remaining variables. The eigenvalue $\lambda \neq 0$ is real and $\mathbf{A}$ is a constant matrix. We assume P, Q and $\mathbf{R}$ and their first derivatives vanish when $(p, q, \mathbf{r}) = (0, 0, \mathbf{0})$. Then, provided $\mathbf{A}$ does not have an eigenvalue which is an integral multiple of λ, there exists a unique invariant two-dimensional local manifold

$$\mathcal{M} = \{(p, q, \mathbf{r}) : |p| + |q| < \delta,\ \mathbf{r} = \mathbf{h}(p, q)\}\,.$$

If we consider all the pairs of variables (p_k, q_k) for which the system equations may be written in the above form, there is a corresponding subcentre manifold for each pair. The space spanned by the union of these manifolds is called the centre manifold.

For the elastic pendulum, there are two such equilibrium points, the elliptic point or centre P_{E} with $(\theta, p_\theta, r, p_r) = (0, 0, (1 + \epsilon_0^2)\ell_0, 0)$ and the hyperbolic point or saddle P_{H} where $(\theta, p_\theta, r, p_r) = (\pi, 0, (1-\epsilon_0^2)\ell_0, 0)$. There is a technical restriction for application of the Lyapunov subcentre manifold theorem: the ratio of the rotational and elastic frequencies must not be an integer ($\omega_{\mathrm{R}}/\omega_{\mathrm{E}} \notin Z$). Subject to this (mild) condition, the theorem implies that there exist *two* local, invariant, two-dimensional manifolds passing through P_{E}. In the neighbourhood of the saddle point, there is one such invariant manifold. One of the local manifolds near P_{E} is obvious:

$$\mathcal{M}_{\mathrm{F}} = \{(\theta, p_\theta, r, p_r) : |r| + |p_r| < \delta_{\mathrm{F}},\ \theta = p_\theta = 0\}\,.$$

This is the fast manifold, representing purely elastic vibrations in the vertical through P_{E}. The Lyapunov result is existential; it ensures that $\mathcal{M}_{\mathrm{F}}$ exists and is unique, but it does not provide an explicit value for δ_{F}. However, it is clear on physical grounds that this fast manifold is actually global; it passes also through the unstable equilibrium point P_{H}. The other invariant manifold near P_{E} is more interesting. The Lyapunov result states that it is of the form

$$\mathcal{M}_{\mathrm{S}} = \{(\theta, p_\theta, r, p_r) : |\theta| + |p_\theta| < \delta_{\mathrm{S}},\ r = f(\theta, p_\theta), p_r = g(\theta, p_\theta)\}\,.$$

The subscript S is chosen more in hope than expectation: the theorem does not imply that this manifold is *slow*. Although the fast variables r and p_r are slaved to θ and p_θ by the functions f and g, there is no guarantee that they do not vary on the fast time-scale.

For the saddle point P_{H} there is no invariant manifold corresponding to $\mathcal{M}_{\mathrm{S}}$. Unlike $\mathcal{M}_{\mathrm{F}}$, which is global (in r and p_r), this manifold may be essentially local in character (confined to a δ-neighbourhood of P_{E}). For $\epsilon = 0$, there is a 2-dimensional centre manifold transverse to 1-dimensional stable

and unstable manifolds around the saddle-point. The theory of normally hyperbolic manifolds (*e.g.*, Wiggins, 1994) guarantees that this structure persists near $P_{\rm H}$ for small perturbations (note that transversality is preserved under diffeomorphism). The fast manifold $\mathcal{M}_{\rm F}$ which we have identified above is identical to the centre manifold. The dynamics near $P_{\rm H}$ are challenging to analyse. Camassa (1995) has investigated this problem for the Lorenz system, using the technique of Melnikov, and has demonstrated the existence of chaos near the hyperbolic point. In a study of a physical system similar but not isomorphic to the elastic pendulum, Georgiou and Schwartz (1996) report the existence of a *global* slow manifold. We have been unable to reach such a conclusion for the system under study here. Indeed, the numerical results presented above strongly suggest that no such global slow manifold exists for the elastic pendulum.

7.3 A Final Thought

First, consider an anelastic pendulum (so that $\epsilon = 0$) at its unstable equilibrium point $P_{\rm H}$ ($\theta = \pi$). If it is disturbed by an infinitesimal impulse of energy δE, it will move away from equilibrium and execute a regular rotational motion of extremely long but constant period, spending most of the time near the top point. Since the initial energy is $E = 1$ and the impulse increases this, the pendulum always has enough energy to surmount the top point on each rotation. The motion is completely predictable.

Now imagine a similar scenario for the elastic pendulum. The bob leaves $P_{\rm H}$ with energy $E = 1 + \delta E$, as before, but now some energy is converted from rotational to elastic oscillations. If the elastic energy $H_{\rm E}$ exceeds δE as the bob approaches $P_{\rm H}$ after a rotation, it will have insufficient energy to reach the top and will fall back. If, on the other hand, $H_{\rm E}$ is less than δE, it will surmount the peak and continue its rotation. But if $H_{\rm E} \approx \delta E$, the course of the pendulum will depend on the phase of the elastic oscillation at the critical angle $\theta = \pi$. For small δE, this will occur long after the initial impulse is applied. On some occasions the bob will surmount the top and on others it will fall back. Although the motion is, in principle, determined by the initial conditions, the precise phase is practically unpredictable; its accurate determination would necessitate keeping track of the phase of the rapid oscillations over a very large number of oscillations—a practical impossibility. The motion will thus have the potential to exhibit high sensitivity to the initial conditions — the signature of chaos.

Acknowledgements

I am sincerely grateful to the organisers of the Programme *Mathematics of Atmosphere and Ocean Dynamics* at the Isaac Newton Institute in Cambridge, for

arranging an excellent research programme. In particular, I wish to thank Ian Roulstone for assistance prior to and during my visit. Several participants in the AOD Programme assisted me in this work, and I gratefully acknowledge the many stimulating and rewarding discussions, and the invaluable guidance to reference material. Special thanks to Onno Bokhove for carrying out all the numerical experiments reported in §5. Finally, I wish to thank the staff of the Isaac Newton Institute, who provided constant support and assistance, contributing greatly to the success of the AOD Programme. My warmest thanks to all of them.

References

Aničin, B A, D M Davidović and V M Babović, 1993: On the linear theory of the elastic pendulum. *Eur. J. Phys.*, **14**, 132–135.

Arnold, V I, 1963: Small denominators and the problem of the stability of motion in classical and celestial mechanics. *Russ. Math. Surv.*, **18**, 85–191.

Arnold, V.I., 1978: *Mathematical Methods of Classical Mechanics.* Springer-Verlag, 508pp.

Arnold, V.I., V.V. Koslov and A.I. Neishtadt, 1988: *Dynamical Systems III. Mathematical Aspects of Classical and Celestial Mechanics.* Springer-Verlag, 291pp.

Banerjee, B and A K Bajaj, 1996: Chaotic responses in two degree-of-freedom systems with 1:2 internal resonances. In *Nonlinear Dynamics and Stochastic Mechanics*, Fields Inst. Comms., **9**, 1–21.

Berry, M.V., 1978: Regular and irregular motion. *Am. Inst. Phys.* Conference Proceedings No. 46: *Topics in Nonlinear Dynamics* pp16–120. (Reprinted in MacKay and Meiss)

Bokhove, O. and T. Shepherd, 1996: On Hamiltonian balanced dynamics and the slowest invariant manifold. *J. Atmos. Sci.*, **53**, 276–297.

Breitenberger, E and R D Mueller, 1981: The elastic pendulum: a nonlinear paradigm. *J. Maths. Phys.*, **22**, 1196–1210.

Burgh, A van der, 1968: On the asymptotic solutions of the differential equations of the elastic pendulum. *J. Mécan*, **7**, 507–520.

Camassa, R., 1995: On the geometry of an atmospheric slow manifold. *Physica D*, **84**, 357–397.

Camassa, R. and S.-K. Tin, 1996: The global geometry of the slow manifold in the Lorenz-Krishnamurthy model. *J. Atmos. Sci*, **53**, 3251–3264.

Carretero-González, R, H N Núñez-Yépez and A L Salas-Brito, 1994: Regular and chaotic behaviour in an extensible pendulum. *Eur. J. Phys.*, **15**, 139–148.

Cayton, Th E, 1977: The laboratory spring-mass oscillator: an example of parametric instability. *Am. J. Phys.*, **45**, 723–732.

Cuerno, R, A F Rañada and J J Ruiz-Lorenzo, 1992: Deterministic chaos in the elastic pendulum: A simple laboratory for nonlinear dynamics. *Am. J. Phys.*, **60**, 73–79.

Curry, S.M., 1976: How children swing. *Am. J. Phys.*, **44**, 924–926.

Daley, R., 1980: The development of efficient time integration schemes using normal mode models. *Mon. Weather Rev.*, **108**, 110–110.

Davidović, D, B A Aničin and V M Babović, 1996: The libration limits of the elastic pendulum. *Am. J. Phys.*, **64**, 338–342.

Diacu, Florin and and Philip Holmes, 1996: *Celestial Encounters: the Origins of Chaos and Stability.* Princeton Univ. Press, 233pp.

Falk, L, 1978: Recurrence effects in the parametric spring pendulum. *Am. J. Phys.*, **46**, 1120–1123.

Georgiou, I.T. and I.B. Schwartz, 1996: The slow invariant manifold of a conservative pendulum-oscillator system. *Intl. J. Bifur. Chaos*, **6**, 673–692.

Heinbockel, J H and R Struble, 1963: Resonant oscillations of an extensible pendulum. *J. Appl. Math. Phys.*, **14**, 262–269.

Hinkelmann, K., 1969: Primitive Equations. Pp. 306–375 in *Lectures in numerical short-range weather prediction.* Regional Training Seminar, Moscow. WMO No. 297.

Holmes, P.J. and J.E.Marsden, 1981: Horseshoes in perturbations of Hamiltonian systems with two degrees of freedom. *Commun. Math. Phys.*, **82**, 523–544.

Jackson, E.A., 1991: *Perspectives of Nonlinear Dynamics*, Vol. I. Cambridge Univ. Press, 496pp.

Jackson, E.A., 1990: *Perspectives of Nonlinear Dynamics*, Vol. II. Cambridge Univ. Press, 633pp.

Kahn, Peter B, 1990: *Mathematical Methods for Scientists and Engineers: Linear and Nonlinear Systems.* John Wiley & Sons. 469pp.

Kane, T R and M E Kahn, 1968: On a class of two-degree-of-freedom oscillations. *J. Appl. Mech.*, **35**, 547–552.

Kelley, A., 1967: On the Liapunov subcenter manifold. *J. Math. Anal. Applic.*, **18**, 472–478.

Kolmogorov, A N, 1954: On the preservation of quasi-periodic motions under a small variation of Hamilton's function. *Dokl. Acad. Nauk. SSSR*, **98**, 525.

Lai, H M, 1984: On the recurrence phenomenon of a resonant spring pendulum. *Am. J. Phys.*, **52**, 219–223.

Landau, L D and E M Lifshitz, 1969: *Mechanics.* Volume 1 of *Course of Theoretical Physics.* Pergamon Press, New York.

Leith, C.E., 1980: Nonlinear normal mode initialization and quasi-geostrophic theory. *J. Atmos. Sci.*, **37**, 958–968.

Lichtenberg, A.J. and M.A. Lieberman, 1992: *Regular and Chaotic Dynamics.* Springer-Verlag, 692pp.

Lorenz, E.N., 1986: On the existence of a slow manifold. *J. Atmos. Sci.*, **43**, 1547–1557.

Lorenz, E.N., 1992: The slow manifold — What is it? *J. Atmos. Sci.*, **49**, 2449–2451.

Lynch, Peter, 1989: The slow equations. *Q. J. Roy. Meteor. Soc.*, **115**, 201–219.

Machenhauer B, 1977: On the dynamics of gravity oscillations in a shallow water model, with applications to normal mode initialization. *Beitr. Phys. Atmos.*, **50**, 253–271

MacKay, R.S. and J.D. Meiss, 1987 *Hamiltonian Dynamical Systems: A Reprint Selection.* Adam Hilger, Bristol.

McLachlan, N W, 1947: *Theory and Application of Mathieu Functions.* Oxford Univ. Press. 401pp.

Minorsky, N, 1962: *Nonlinear Oscillations.* Van Nostrand, Princeton. p506.

Moser, J, 1962: On invariant curves of area-preserving mappings on an annulus. *Nachr. Akad. Wiss. Göttingen Math. Phys.*, **K1**, 1.

Moser, Jürgen, 1978: Is the solar system stable? *Math. Intelligencer*, **1**, 65–71 (Reprinted in MacKay and Meiss).

Nayfeh, A.H., 1973: *Perturbation Methods.* John Wiley & Sons, Inc., 425pp.

Núñez-Yépez, H N, A L Salas-Brito, C A Vargas and L Vicente, 1990: Onset of chaos in an extensible pendulum. *Phys. Lett.*, **A145**, 101–105.

Olsson, M G, 1976: Why does a mass on a spring sometimes misbehave? *Am. J. Phys.*, **44**. 1211-1212.

Ott, Edward, 1993: *Chaos in Dynamical Systems.* Cambridge Univ. Press, 385pp.

Paulling, J R and R M Rosenberg, 1959: On unstable ship motions resulting from nonlinear coupling. *J. Ship Res.*, **June, 1959**, 36–46.

Percival, I and D Richards, 1982: *Introduction to Dynamics.* Cambridge Univ. Press, 228pp.

Peterson, Ivars, 1993: *Newton's Clock: Chaos in the Solar System.* W. H. Freeman, New York, 317pp.

Press, W.H., S.A. Teukolsky, W.T. Vetterling and B.P. Flannery, 1992: *Numerical Recipes in C.* Cambridge Univ. Press.

Rusbridge, M G, 1980: Motion of the spring pendulum. *Am. J. Phys.*, **48**, 146–151.

Richardson, L.F. and J.A. Gaunt, 1927: The deferred approach to the limit. *Phil. Trans. Royal Soc.*, **A226**, 299–361.

Tabor, Michael, 1989: *Chaos and Integrability in Nonlinear Dynamics.* John Wiley & Sons, New York, 364pp.

Vitt, A and G Gorelik, 1933: Swinging of an elastic pendulum as an example of two parametrically coupled linear oscillation systems. *Zh. Tekh. Fiz.* (*J. Tech. Phys.*) **3**(2-3), 294–307. (In Russian; English translation available from Met Éireann).

Wells, David, 1991: *The Penguin Dictionary of Curious and Interesting Geometry.* Penguin Books, 285pp.

Weissert, Thomas P, 1997: *The Genesis of Simulation in Dynamics: Pursuing the Fermi-Pasta-Ulam Problem.* Springer, 176pp.

Wiggins, S., 1994: *Normally Hyperbolic Invariant Manifolds in Dynamical Systems.* Springer-Verlag, New York, 193pp.

Yoshida, H., 1990: Construction of higher order symplectic integrators. *Phys. Lett. A*, **150**, 262–268.

Figure Captions

Fig. 1. (a) Elastic pendulum in equilibrium. Mass of bob m, stretched length ℓ, stiffness of wire k. (b) Pendulum in motion, polar coordinates (r, θ).

Fig. 2. Limaçon curves for $\epsilon_0 \in \{0.1, 0.4, 0.7, 1.0\}$ ($\epsilon_0 = 1$ gives a cardioid). Unit circle shown dashed.

Fig. 3. Surface $\mathcal{S}_1$ ($\epsilon = 0.25$) upon which the solutions of the slow equations (12) evolve. Note that $p_r \equiv 0$.

Fig. 4. Numerical solutions. LIN: linear initialization, NLI: nonlinear initialization, SLO: slow equations. For more details, see text.

Fig. 5. Phase diagram for the simple pendulum. A pair of homoclinic orbits joining the unstable equilibrium point $\theta = \pm\pi$ to itself form the separatrix, dividing the phase-plane into regions of libration and regions of clockwise and anticlockwise rotation.

Fig. 6. Poincaré sections for twelve trajectories with total energy $E = 0.0$. Top two rows: $\epsilon \in \{0.025, 0.05, 0.1\}$ (slow plane in first row, fast plane in second). Bottom two rows: $\epsilon \in \{0.25, 0.325, 0.4\}$ (slow plane in third row, fast plane in fourth).

Fig. 7. Poincaré sections for twelve trajectories with total energy $E = 1.8$. Top two rows: $\epsilon \in \{0.025, 0.05, 0.1\}$ (slow plane in first row, fast plane in second). Bottom two rows: $\epsilon \in \{0.25, 0.325, 0.4\}$ (slow plane in third row, fast plane in fourth).

Fig. 8. Equipotential lines of the swinging spring near the point of stable equilibrium.

Fig. 9. Amplitudes of the horizontal or swinging component (solid) and of the vertical or springing component (dashed) for the case of resonance. Panel (a) is for the smaller energy ($z(0) = 0.05$). Panel (b) is for the larger energy ($z(0) = 0.1$).

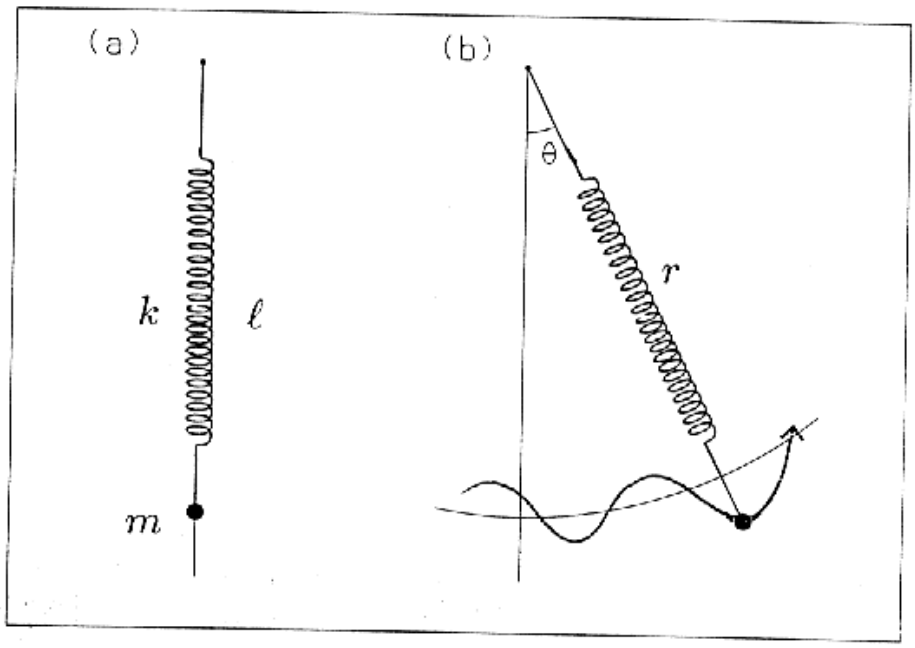

Fig. 1. (a) Elastic pendulum in equilibrium. Mass of bob m, stretched length ℓ, stiffness of wire k. (b) Pendulum in motion, polar coordinates (r, θ).

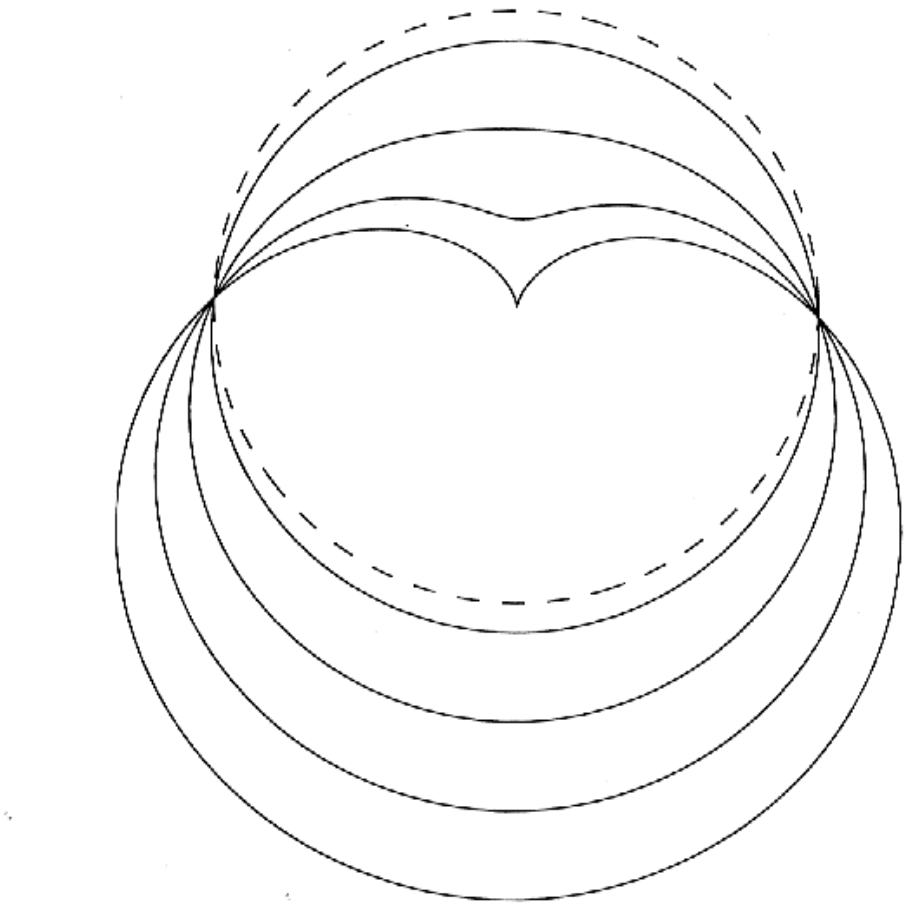

Fig. 2. Limaçon curves for $\epsilon_0 \in \{0.1, 0.4, 0.7, 1.0\}$ ($\epsilon_0 = 1$ gives a cardioid). Unit circle shown dashed.

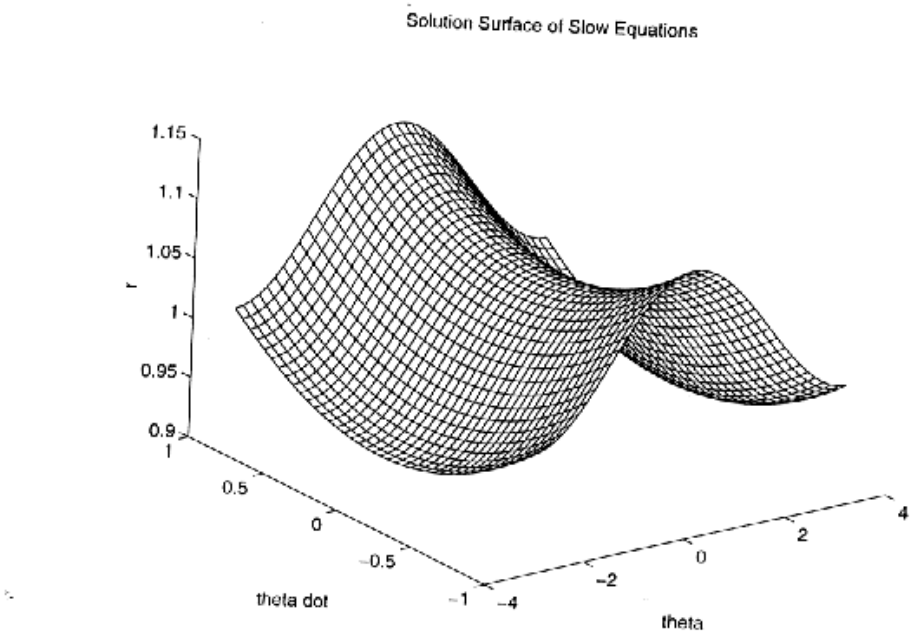

Fig. 3. Surface $\mathcal{S}_1$ ($\epsilon = 0.25$) upon which the solutions of the slow equations (12) evolve. Note that $p_r \equiv 0$.

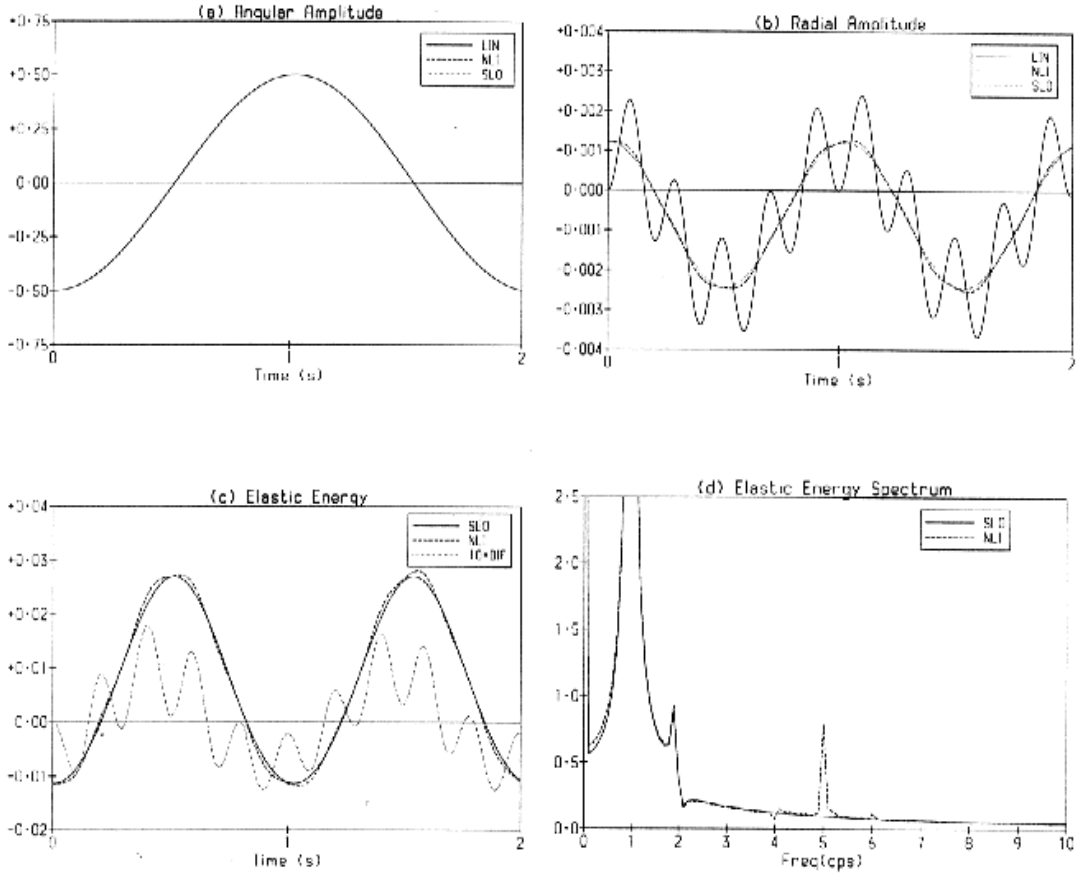

Fig. 4. Numerical solutions. LIN: linear initialization, NLI: nonlinear initialization, SLO: slow equations. For more details, see text.

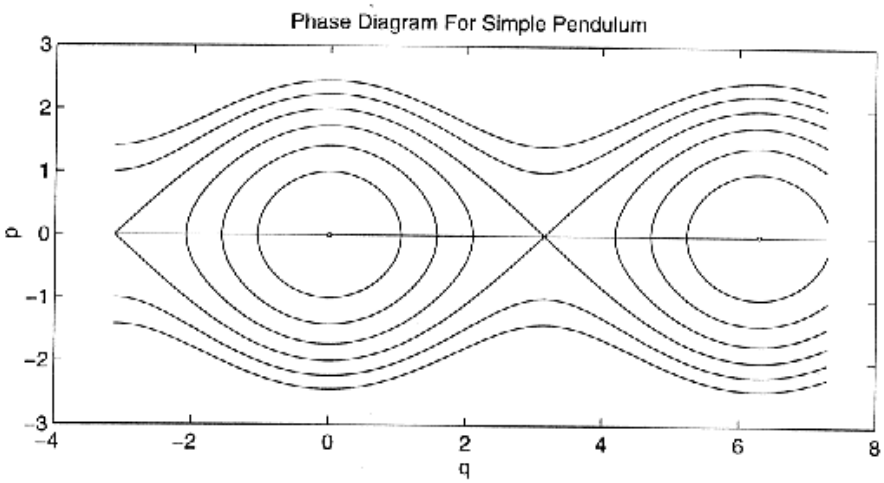

Fig. 5. Phase diagram for the simple pendulum. A pair of homoclinic orbits joining the unstable equilibrium point $\theta = \pm\pi$ to itself form the separatrix, dividing the phase-plane into regions of libration and regions of clockwise and anticlockwise rotation.

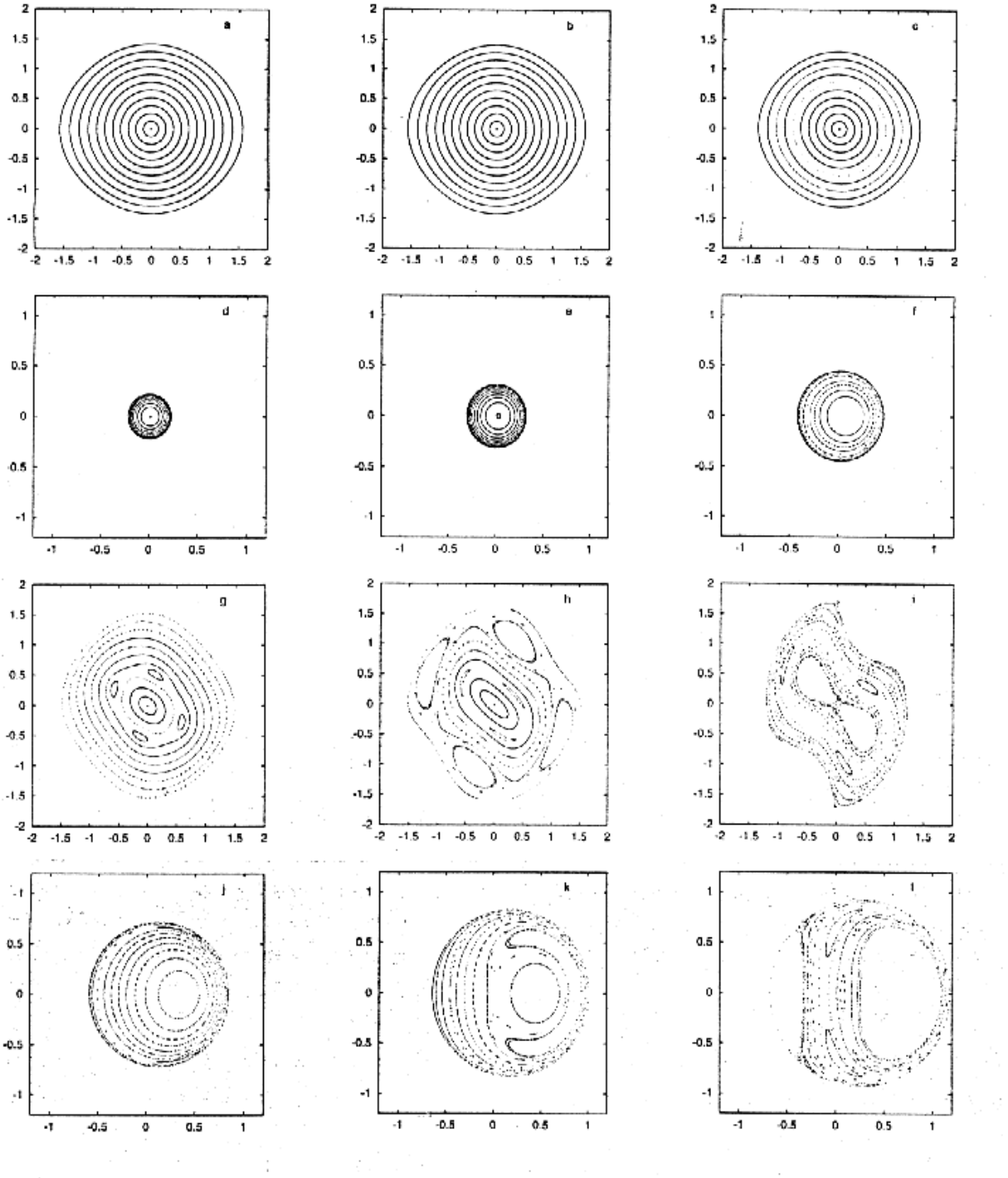

Fig. 6. Poincaré sections for twelve trajectories with total energy $E = 0.0$. Top two rows: $\epsilon \in \{0.025, 0.05, 0.1\}$ (slow plane in first row, fast plane in second). Bottom two rows: $\epsilon \in \{0.25, 0.325, 0.4\}$ (slow plane in third row, fast plane in fourth).

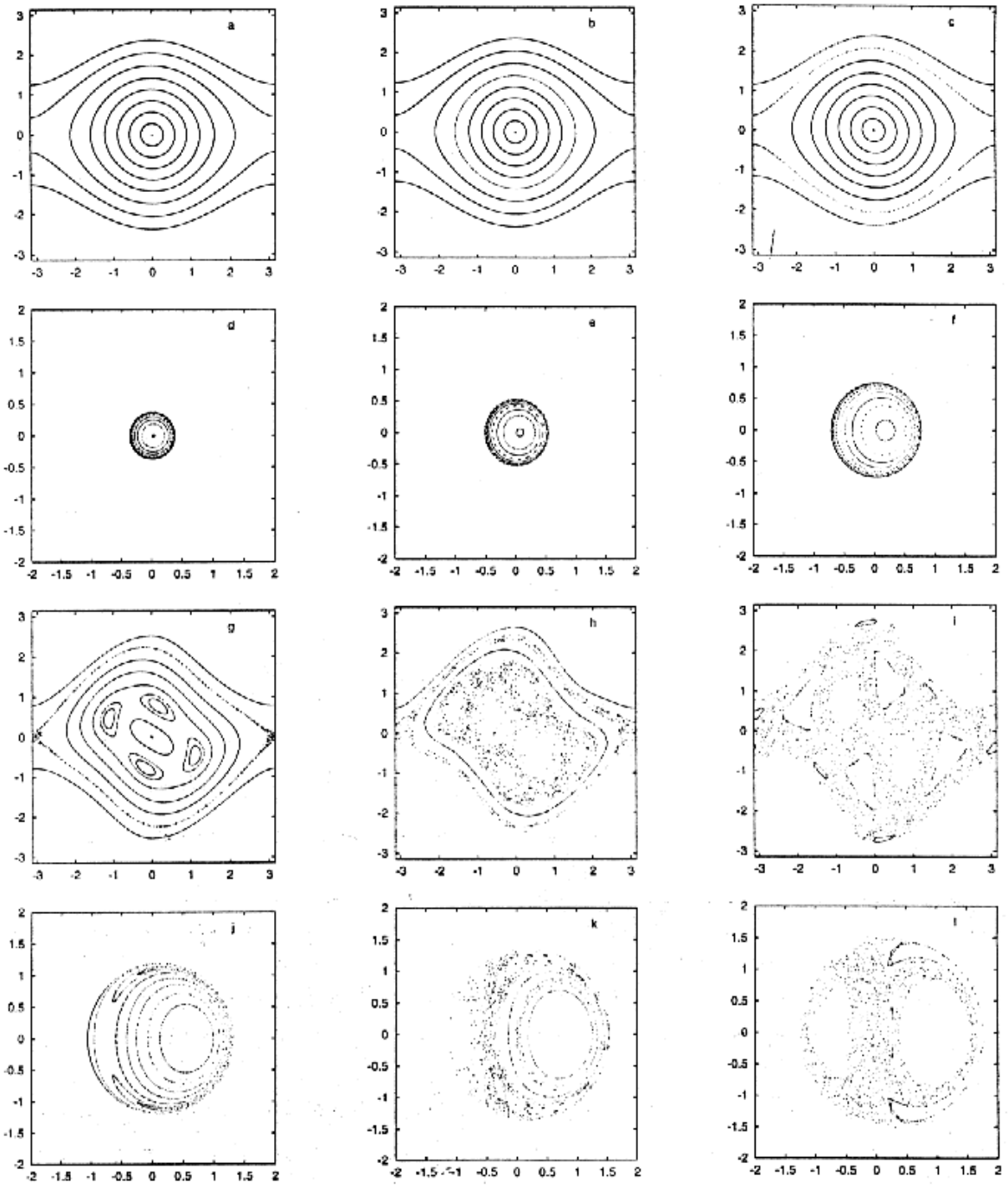

Fig. 7. Poincaré sections for twelve trajectories with total energy $E = 1.8$. Top two rows: $\epsilon \in \{0.025, 0.05, 0.1\}$ (slow plane in first row, fast plane in second). Bottom two rows: $\epsilon \in \{0.25, 0.325, 0.4\}$ (slow plane in third row, fast plane in fourth).

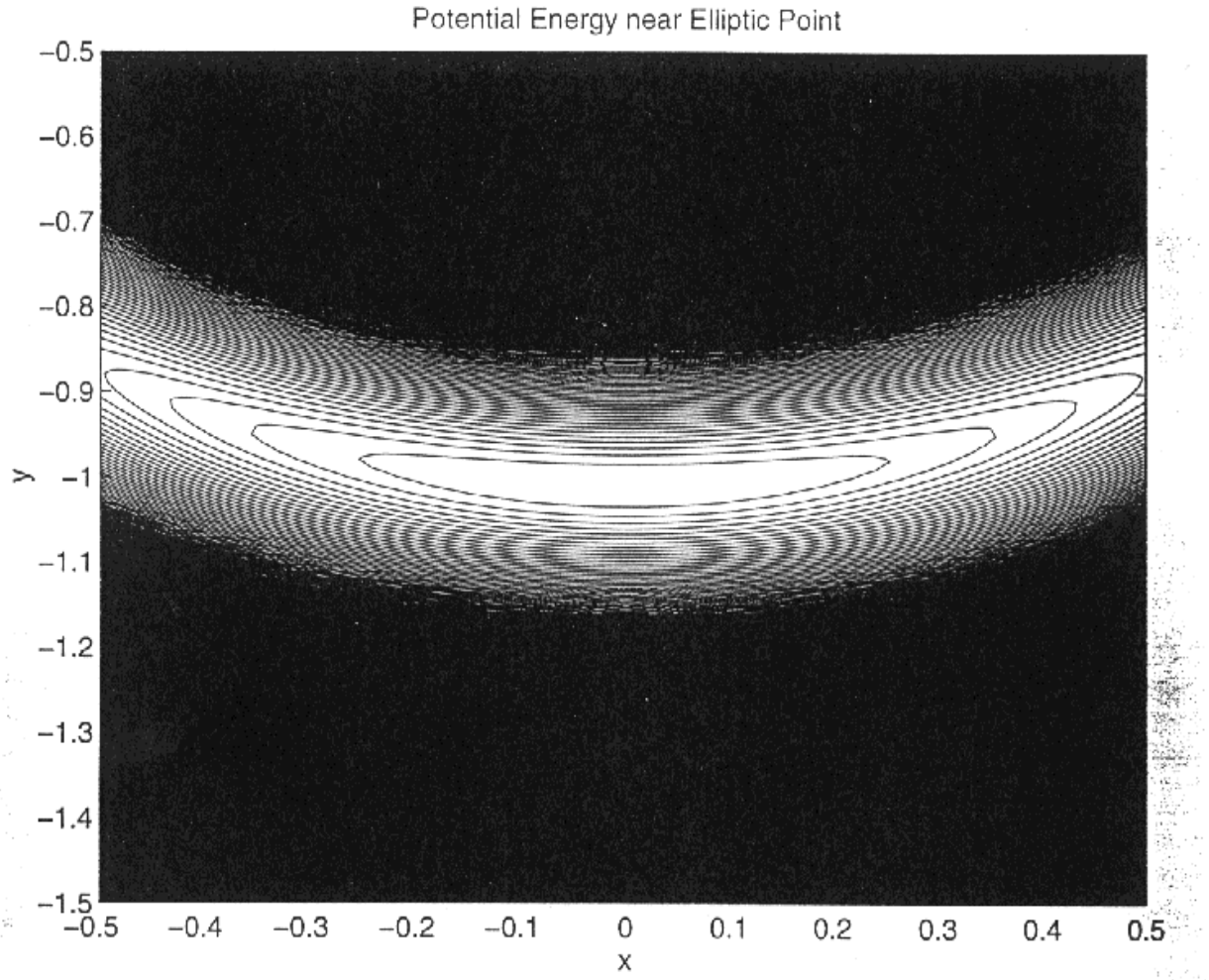

Fig. 8. Equipotential lines of the swinging spring near the point of stable equilibrium.

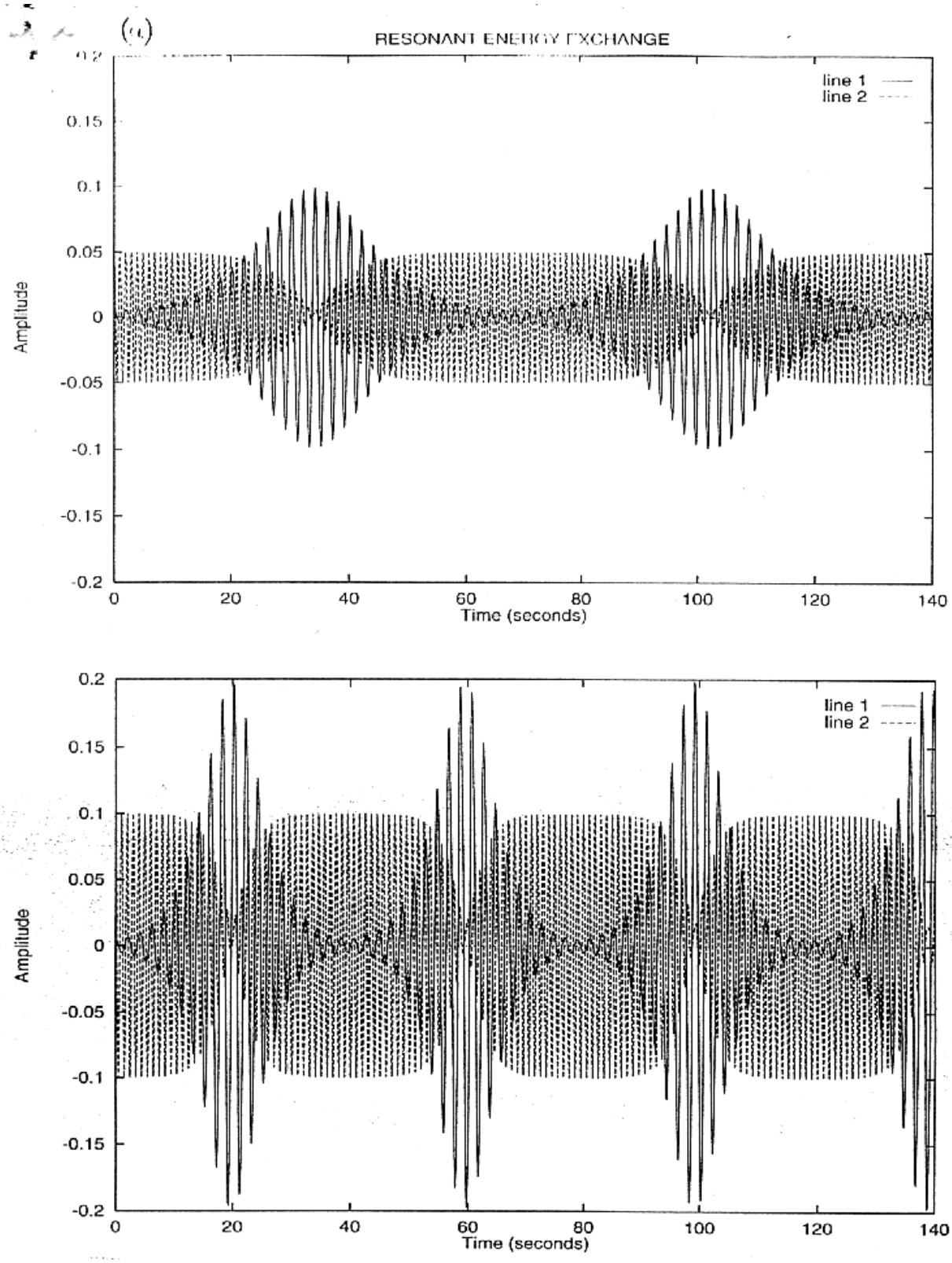

Fig. 9. Amplitudes of the horizontal or swinging component (solid) and of the vertical or springing component (dashed) for the case of resonance. Panel (a) is for the smaller energy ($z(0) = 0.05$). Panel (b) is for the larger energy ($z(0) = 0.1$).